Codeposition and Plasma Interaction with Codeposited/Mixed Materials

J. W. Davis

University of Toronto Institute for Aerospace Studies

Outline

1) INTRODUCTION:
   - General introduction to codeposition in tokamaks
   - Materials involved in Codeposition
   - Implications of codeposition in ITER and future reactors

2) IMPURITY TRANSPORT IN TOKAMAKS:
   - Impurity sources
   - Neutral transport
   - Plasma transport
   - Codeposition patterns in JET, DIII-D

3) TOKAMAK FILM CHARACTERIZATION:
   - Modified surface layers
   - Carbon films
   - Tokamak codeposits
   - Codeposition with beryllium
   - Codeposition with Tungsten

Outline (continued)

4) PLASMA INTERACTION WITH CODEPOSITS AND MIXED MATERIALS:
   - Erosion of a-C:H films
   - Erosion of bulk mixed materials
   - Modified/mixed surfaces

5) REMOVAL OF CODEPOSITED FILMS:
   - T removal from JET and TFTR
   - Removal of codeposited films by oxidation
   - Oxidation Experiments in TEXTOR, HT-7 and ASDEX
   - Surface heating techniques
   - Mechanical scrubbing

6) CONCLUSIONS:

1. Introduction

1.1 General introduction to codeposition in tokamaks

1.2 Materials involved in codeposition

1.3 Implications of codeposition in ITER and future reactors

1.1 General Introduction to Codeposition in Tokamaks

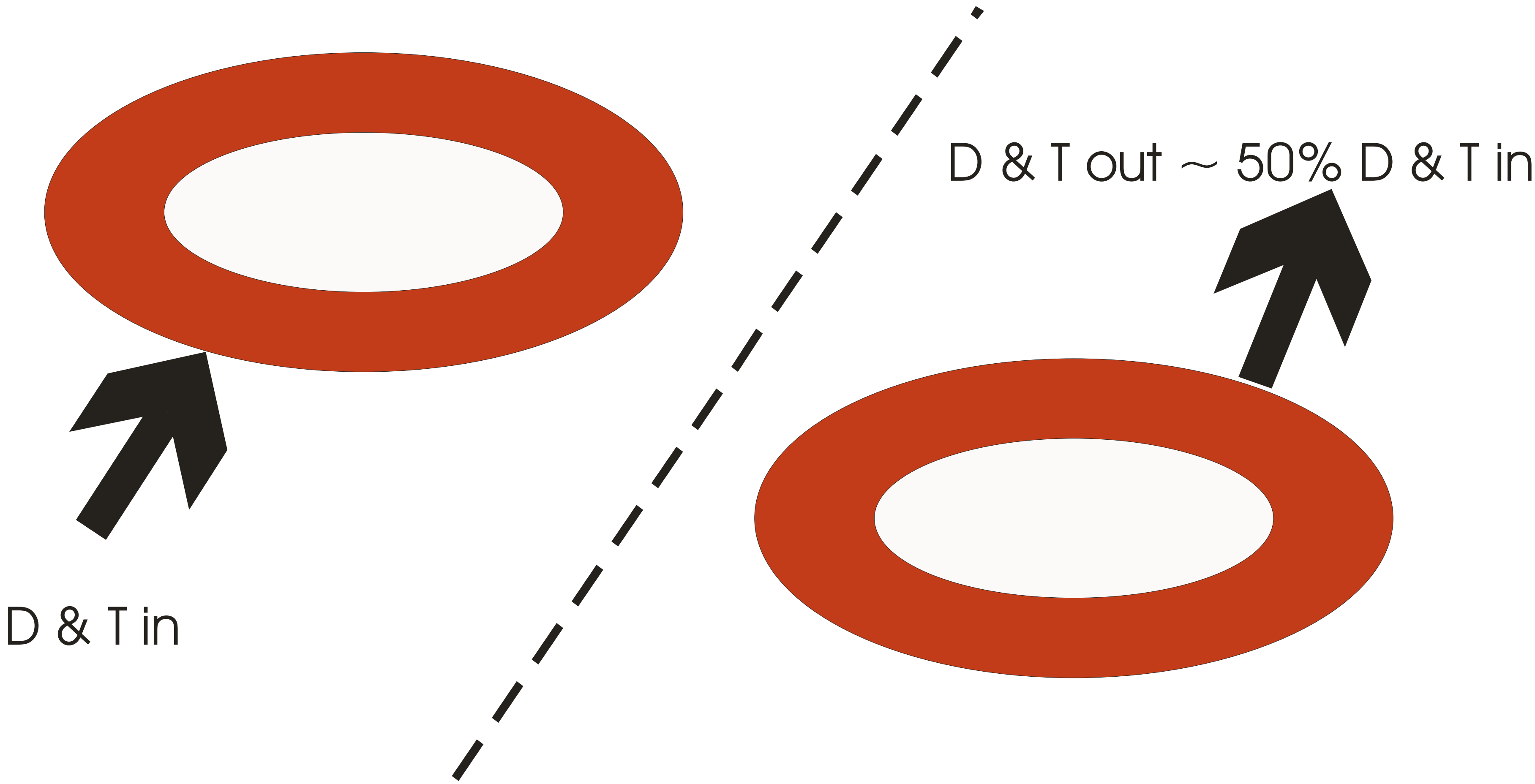

Where does all this D go?

Particle Sources and Radiation from Fusion Plasmas

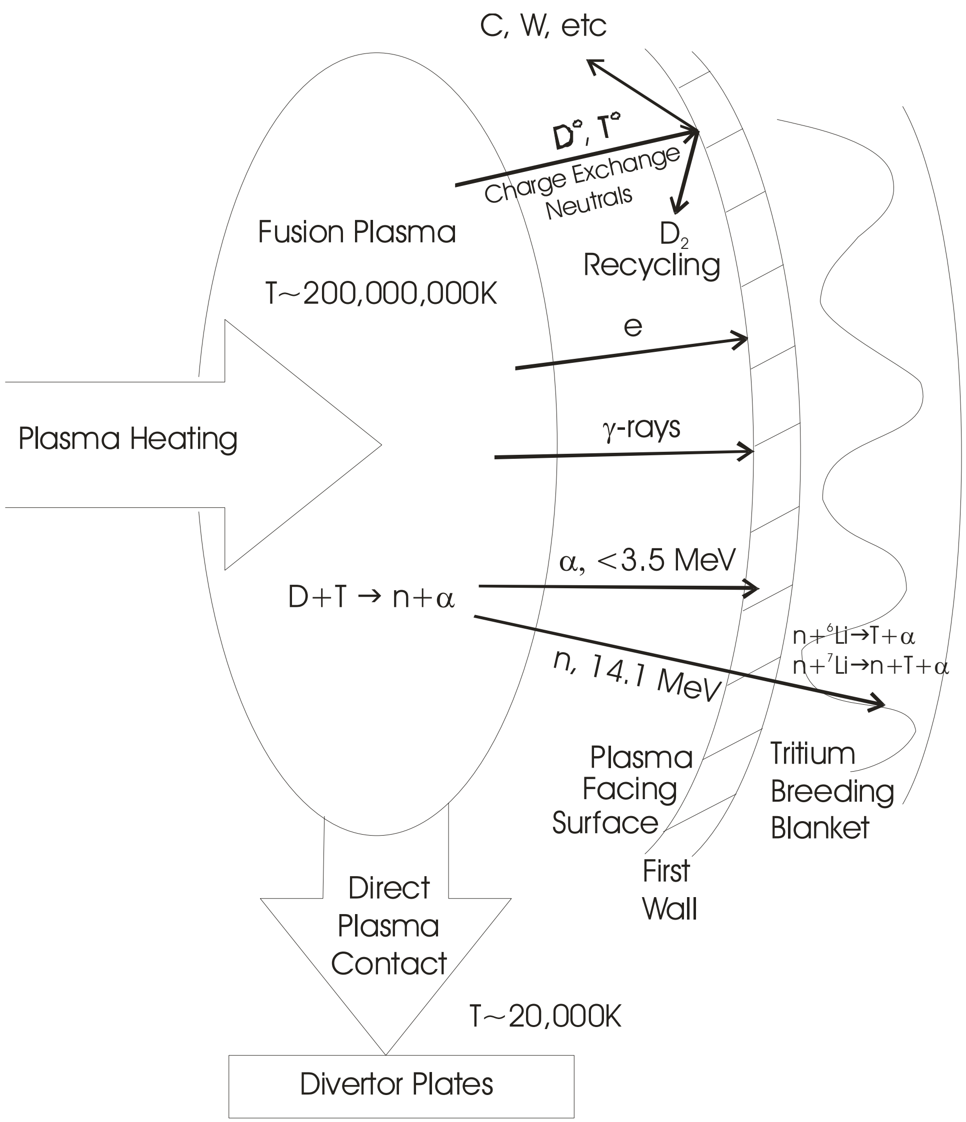

- Next to a fusion plasma is a very hostile environment
- All plasma-facing surfaces will be subject to both erosion and deposition.
- Codeposition involves the erosion of impurity atoms and their deposition (along with hydrogen).

Impurity Particle Balance

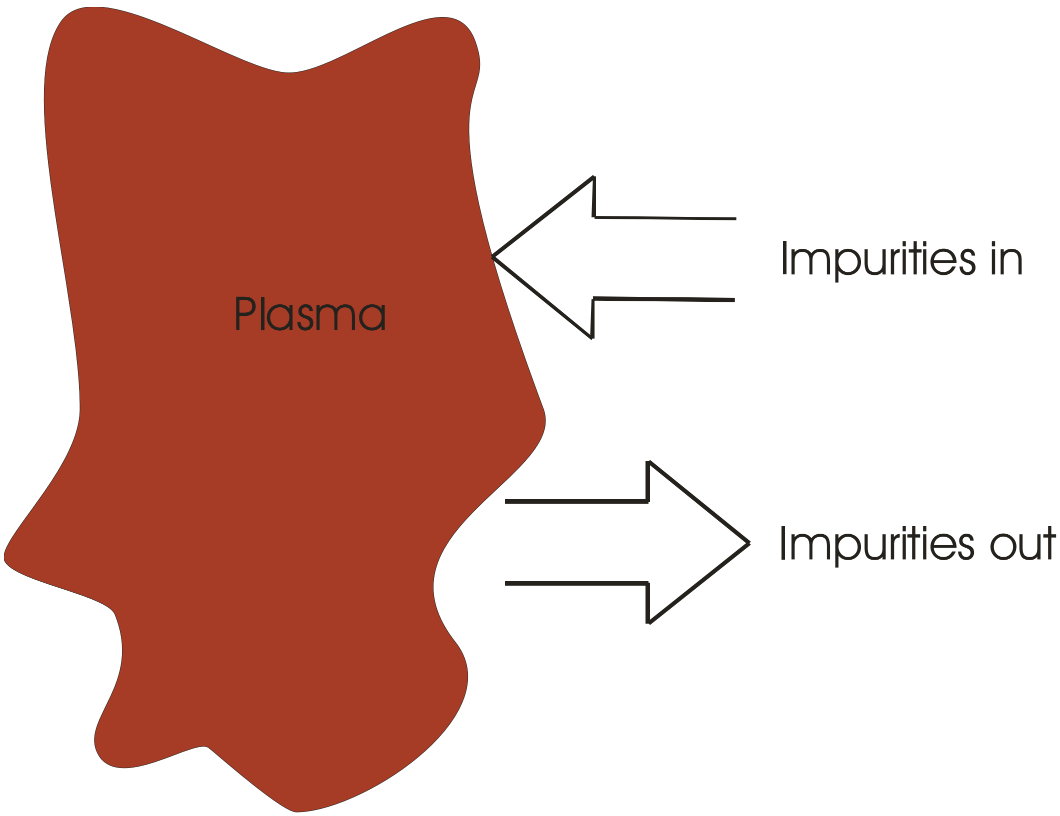

- In long pulse devices, near-steady-state conditions will develop:

  $\Rightarrow$ Impurities in = impurities out

- In fact, most impurities will never make it to the core plasma, but will be ionized in the periphery, and return to a plasma-facing surface.

Impurity Transport 1

- Now, impurity atoms leaving the plasma do not generally return to their original location.

- Several transport mechanisms are involved in determining exactly where such atoms will finally end up once they have been removed from a plasma-facing surface.

$\Rightarrow$ neutral transport into the plasma

$\Rightarrow$ transport as impurity ions

$\Rightarrow$ possible neutral transport to non-plasma-contact surfaces

Impurity Transport 2

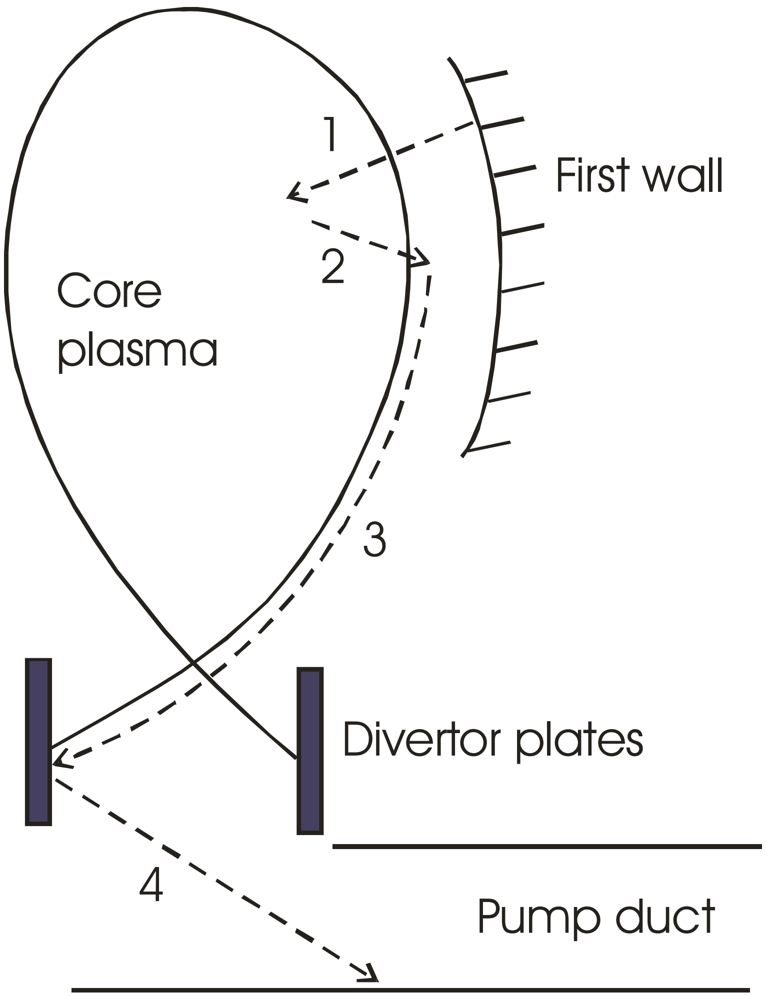

Possible Impurity Particle Path:

1) Sputtering off main chamber first wall and transport as neutral until ionization in main plasma

2) Diffusion from main plasma to scrape off layer

3) Transport along scrape off layer to divertor plate

4) Removal from divertor plate, and transport as neutral to pump duct

Codeposition 1

- The primary factors which control the deposition process are:
  - impurity/hydrogen ratio in the incident flux
  - surface temperature
  - ion/neutral particle energy

- Regions where codeposited layers accumulate can vary widely between different machines, and even for the same machine under different operating conditions.

- Some reactor surfaces, while line-of-sight to the plasma, do not receive a significant ion/plasma flux due to the shielding effect of the magnetic field.
  - Such surfaces, like the pump duct of the previous slide, or gaps between tiles, may still receive a significant flux of sputtered neutrals (impurities) and charge-exchange neutrals (hydrogen) or Franck-Condon atoms.

Codeposition 2

- In regions adjacent to the divertor, the energy of the majority of charge-exchange neutrals may be too low to cause significant physical sputtering, although chemical reactions are still possible.
  - It is very difficult to predict where codeposition might occur.

- Because of the large flux of hydrogen which is incident on all surfaces, hydrogen is often trapped in the accumulating films; the layers contain a mixture of hydrogen and impurity atoms:

  $\Rightarrow$ **Codeposition**

- And this is where we believe most of the "missing" hydrogen will be found.

1.2 Materials Involved in Codeposition

- Current tokamaks are largely dominated by carbon impurities, even if they do not have carbon-based materials as the primary plasma-facing material.
- Disadvantages of carbon:
  - Light element, fairly high sputtering yield.
  - Chemically reactive to hydrogen.
  - Ideal for forming hydrocarbon layers.

$\Rightarrow$ Carbon films are used in industry for a wide variety of purposes.

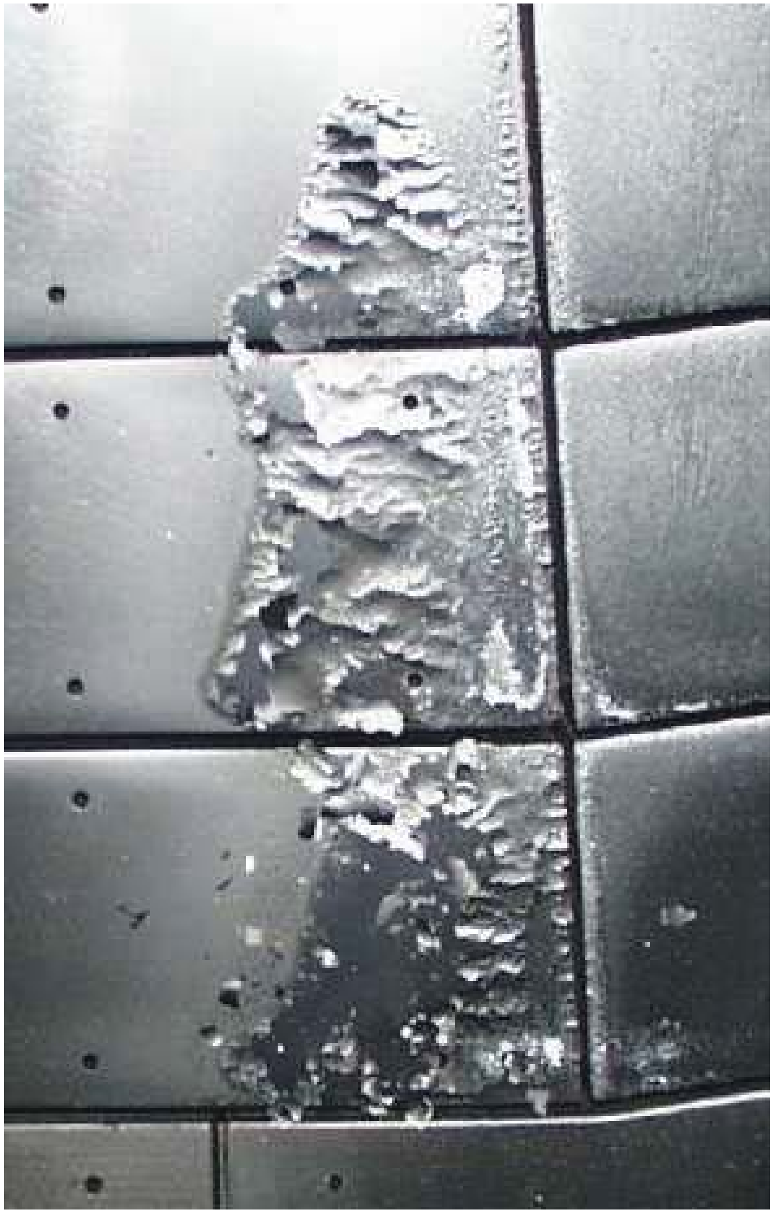

- These features have led to carbon being deposited with D in increasingly thick layers at various locations in the tokamak

- While the films may have a limit to the thickness attained before flaking occurs, the deposition process is non-limiting.

- Photo is from TFTR (Federici, 2001)

Materials in ITER

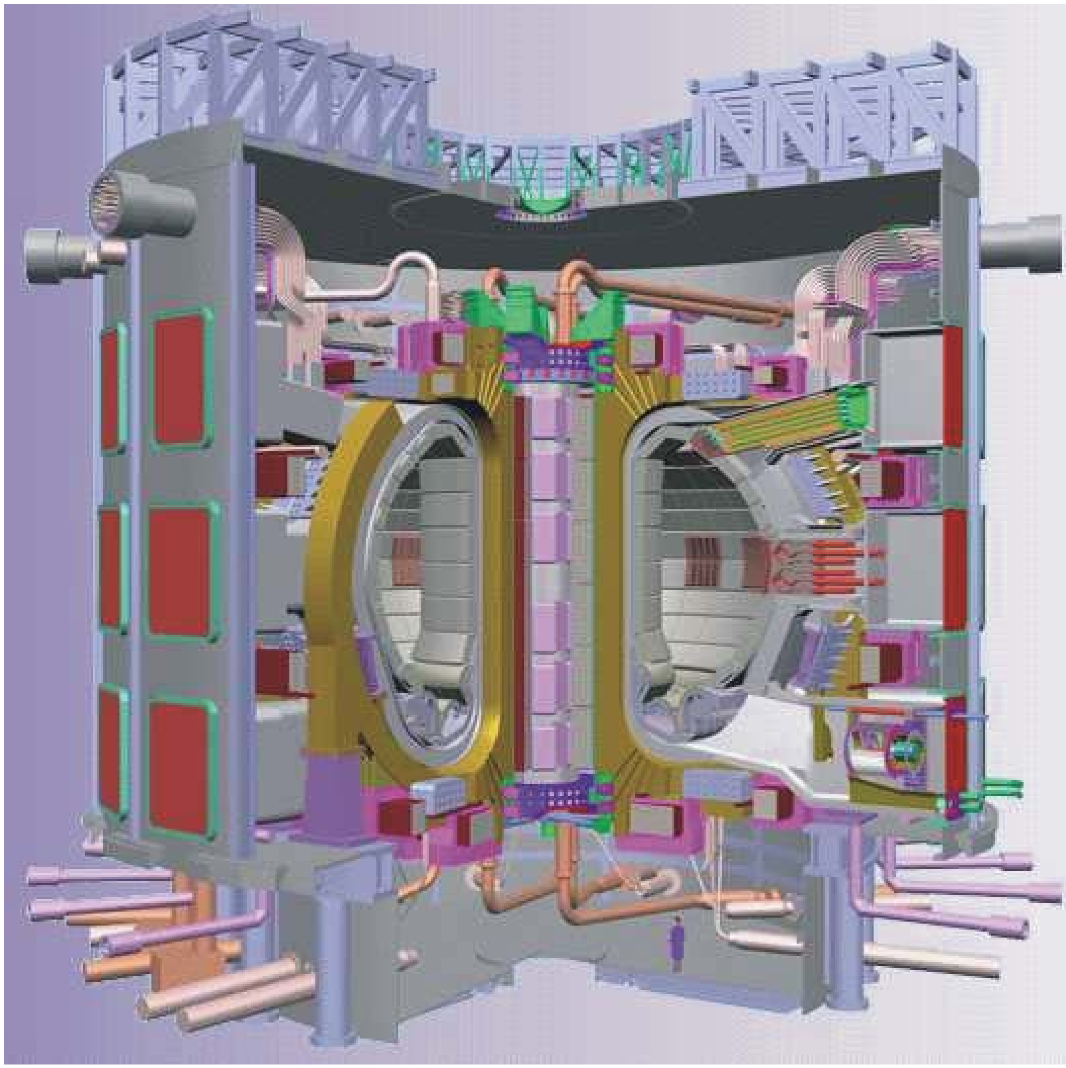

- Current plans call for:
  - ⇒ Be first wall
  - ⇒ W divertor region
  - ⇒ C divertor plates
- Inevitably, there will be substantial cross-contamination of all surfaces.

Codeposition with Be and W

- Pure Be and pure W have very low hydrogen solubility, and thus are not likely to trap significant amounts of tritium.

- However, the structure of the deposit may incorporate large numbers of trapping sites.

- In addition, both Be and W form stable oxides, carbides and hydroxides which do trap hydrogen, and thus they have the ability to form codeposited layers.

- The properties of mixed material codeposits are mostly unknown.

- Metallic codeposits may be more difficult to remove than carbon-based codeposits.

1.3 Implications of codeposition in ITER

- ITER will be limited to an on-site tritium inventory of about 4000 g
- Mobilizable (in-vessel) inventory is limited to 350 g (1000 g?).
- Once this second limit is reached, ITER will be required to stop running tritium discharges until part, or all, of the tritium has been recovered from the torus.
- Clearly, it is desirable that this happen as infrequently as possible.

Codeposition in ITER

- Want 10,000 full power shots, 400 s long.

- Calculations give about 4 g tritium retained per shot (Federici, 2003).

$\Rightarrow$ 90 shots! (5 – 10 days of operation)

- Codeposits must then be removed before further operation is allowed.

- Permanent retention: 350 g/10,000 shots = 0.035 g/shot

$\Rightarrow$ **removal must be > 99% effective!**

Codeposition in a Power-Generating Reactor 1

- In a fusion power reactor, aside from tritium inventory, there is also the issue of tritium self-sufficiency. The loss rate of tritium must be small enough that the reactor can still produce as much tritium as it needs to operate.

- Generally accepted value for tritium breeding ratio (TBR): 1.1 T/neutron

- Only a small fraction of the tritium in the reactor will undergo fusion:

  $\Rightarrow$ pumping required to remove He ash

  $\Rightarrow$ Maximum He concentration in plasma ~ 10%

  $\Rightarrow$ Relative pumping efficiency, helium/hydrogen ~ 20%

Codeposition in a Power-Generating Reactor 2

- The rate at which He is pumped out is equal to the rate at which T is consumed.

$\therefore$ T flow through / T consumed $= 1 / (0.10 \times 0.20 \times 2) = 25$

$\Rightarrow$ On average, 4% of the tritium injected into the reactor will undergo fusion

$\therefore$ Maximum allowable loss rate $= 4\% \times (\text{TBR} - 1) = 0.4\%$

$\Rightarrow$ probably need loss rate < 0.1% due to other losses

- **A power-generating reactor will simply not be able to tolerate codeposition.**

Codeposition Summary

- Currently, 30 – 50% of hydrogen admitted to fusion reactors remains in the reactor.

- After extensive cleaning procedures, this has been reduced to a few %.

- For ITER to successfully complete the desired program of operation, the amount remaining in the vessel after cleaning must be < 0.1%.

- For a commercial reactor, the fraction of tritium retained must be < ~ 0.1% for tritium self-sufficiency, and also for T inventory considerations.

2. Impurity Transport in tokamaks

2.1 Impurity sources

2.2 Neutral transport

2.3 Plasma transport: 1D SOL model

2.4 Codeposition patterns in JET

2.5 Codeposition patterns in DIII-D

2. Impurity Transport in Tokamaks

- The formation of codeposited layers is fundamentally tied to the transport of materials from one location in a tokamak to another.

- In this section, we will have a look at several issues related to this transport:

  $\Rightarrow$ Impurity sources

  $\Rightarrow$ Impurity transport as neutrals and as ions

2.1 Impurity Sources

- One would expect that the areas of the tokamak plasma-facing surfaces which receive the most flux would be the largest sources of impurities entering the core plasma. However, the importance of impurity sources on core contamination depends on many factors:

  - magnetic geometry
  - proximity of the surface to the core plasma
  - adjacent plasma conditions (temperature, density)
  - plasma flux to the surface (composition)

Tokamak Magnetic Geometry

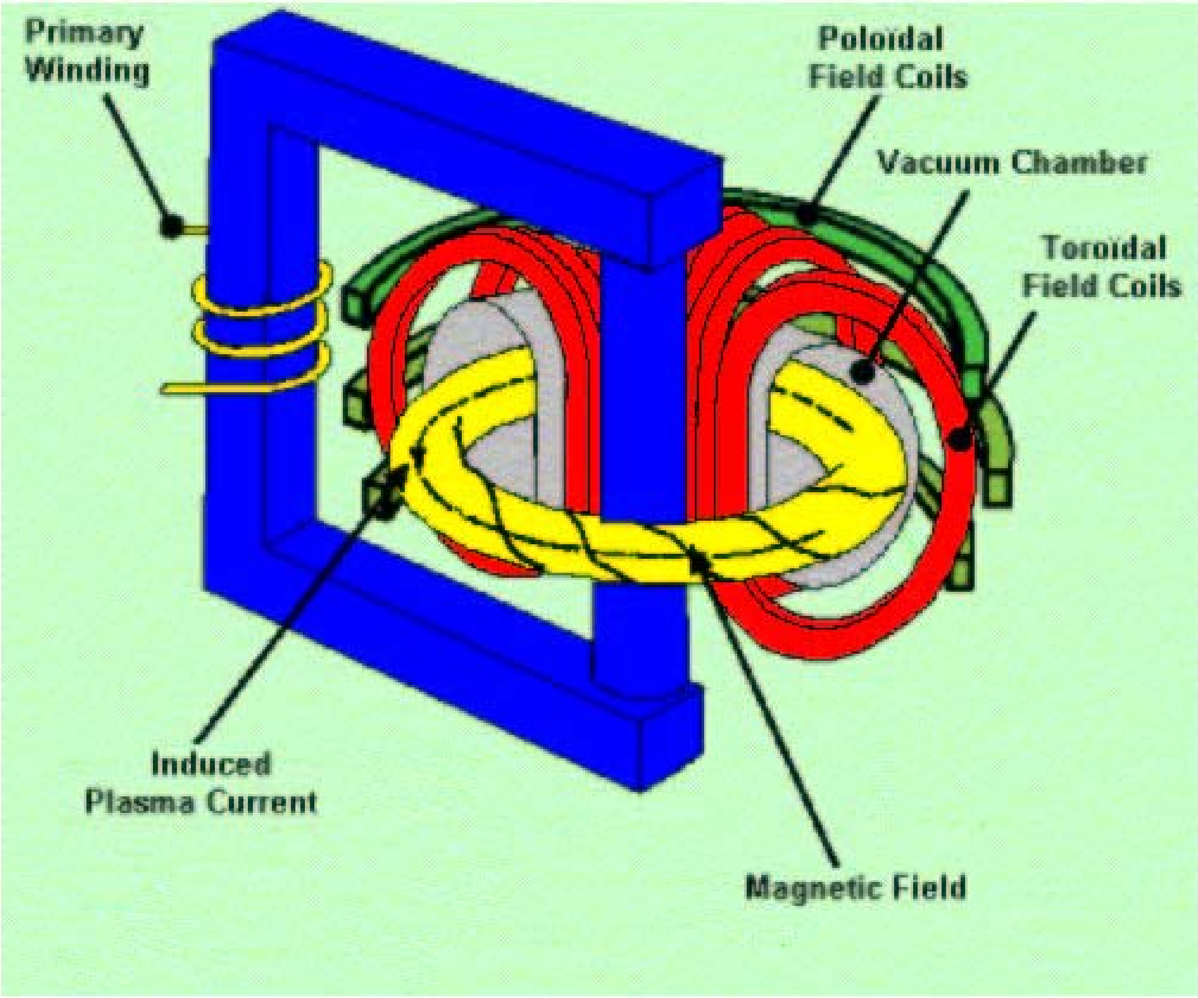

Limiter geometry:

- Plasma contacts solid surface at boundary with core plasma.
- Impurities may be released directly inside Last Closed Flux Surface (LCFS).
- Examples: TFTR, Tore Supra , TEXTOR, HT-7

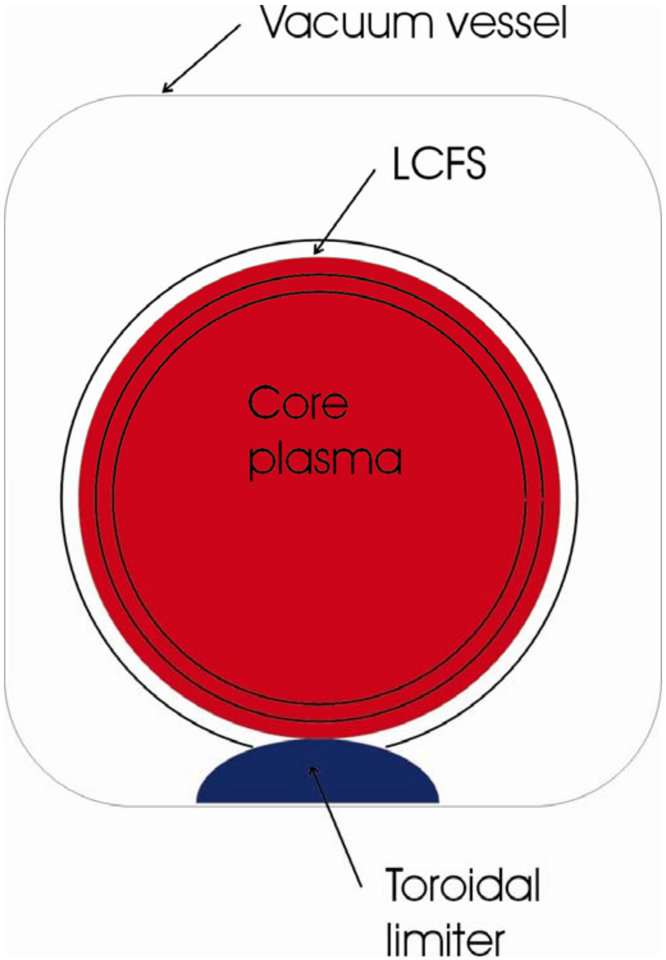

Divertor Geometry

- Plasma contact on surfaces physically removed from core plasma; however, still close magnetically
- Impurities released from divertor plates must travel longer distances as neutrals to reach plasma
- Examples: JET, ASDEX, DIII-D, C-mod

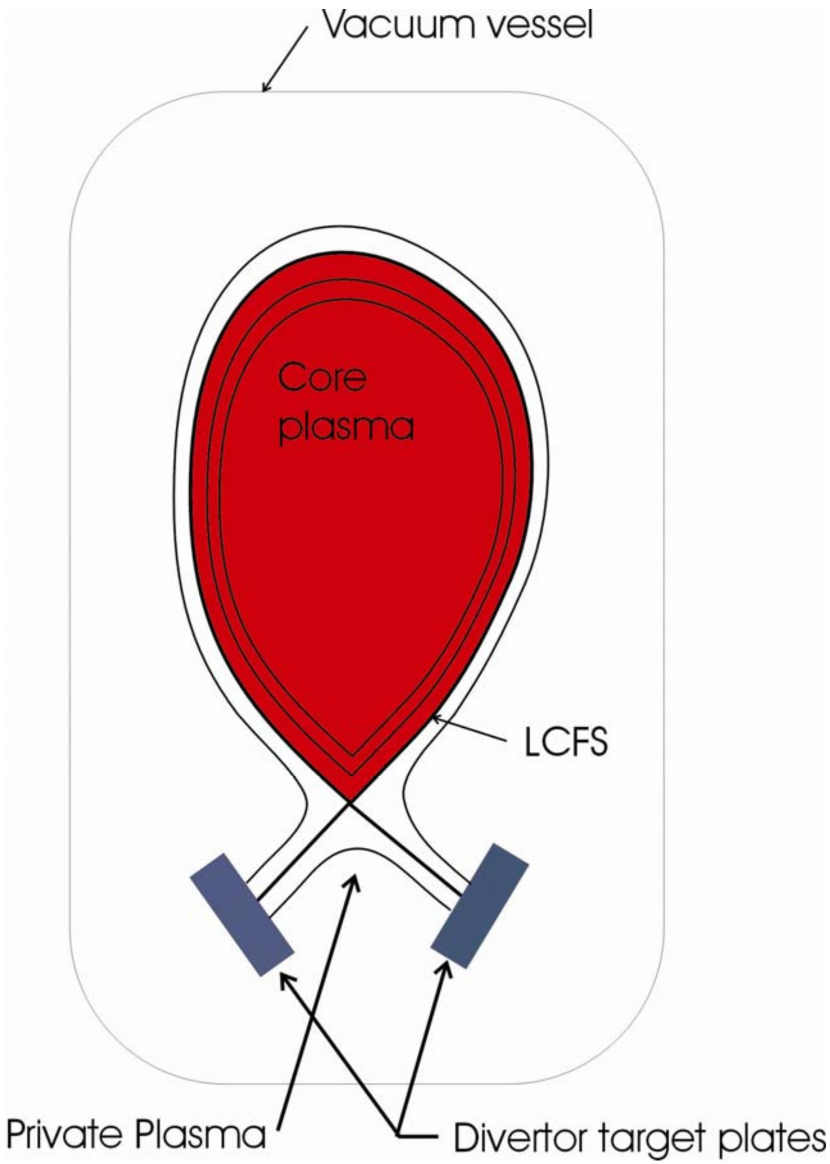

- The limiter and divertor geometries represent fundamentally different methods for control of plasma-surface interactions.

- To give an idea of the complexity of such systems, it has yet to be demonstrated conclusively that divertor machines are inherently cleaner than limiter machines.
  – It does appear, however, that divertor tokamaks have advantages with regard to power loading, particularly under detached conditions.

- Clearly our current state of understanding of impurity transport in tokamaks is inadequate, and there is a lot of effort directed toward improving this situation.
  – See PPI presentation

- For our discussion, we will first look at the different sources of impurities, and then focus on the transport mechanisms.

Impurity Sources: First Walls

- First walls, not in the vicinity of the divertor, are generally 5-50 cm back from the LCFS.

- Since the plasma density and temperature decrease exponentially outside the LCFS, with a scale length of a few cm, the conventional view is that the walls will experience very little plasma contact during normal operation.

- Most erosion would then be due to charge-exchange neutrals, which are able to cross the magnetic field lines

  $\Rightarrow$ fluxes $\sim 10^{20}$ H/m^{2}s

  $\Rightarrow$ energies up to a few keV

- More recent analysis indicates that there may be more substantial plasma contact, and hence more erosion.

Impurity Sources: Divertor Plates

- Divertor plates are the regions of most intense plasma contact.

- ITER likely to operate with “high density” or detached divertor plasma:

  $\Rightarrow$ plasma temperature few eV

  $\Rightarrow$ volume recombination of hydrogen important

  $\Rightarrow$ particle flux to divertor plates ~ 10^{22} – 10^{23} D/m^{2}s

- Neutral particles sputtered from divertor plates have a high probability of not being directed toward the core plasma.

- Impurities also have a large probability of being ionized close to the surface and being redeposited nearby.

Impurity Sources: Divertor Region

- The region around the divertor plates, and in the private plasma region, will see plasma conditions intermediate to the first wall and divertor target plates.

- Some areas are likely to be regions of net deposition, while others are likely to be regions of net erosion.

2.2 Neutral Transport

- The great majority of erosion-produced impurity atoms and molecules (> 90%) will leave their surface of origin as neutral particles.

- Thus their initial motion will be unaffected by the magnetic field.

- Processes affecting particle motion:

  $\Rightarrow$ ionization

  $\Rightarrow$ dissociation

  $\Rightarrow$ elastic collisions

Physically Sputtered Neutrals

- The majority of physically sputtered particles are released as individual atoms.
- Multi-atom clusters, eg., CH, C_2 or C_3 are also released.
- Energy of particles released given by Thompson Distribution, with typical energies of a few eV (Thompson, 1968).
- Particles are released with approximately a cosine distribution, meaning that the probability of a particle being released into a solid angle $d\omega$ is proportional to the cosine of the angle θ to the surface normal (Greenwood, 2002). Most probable angle = 45°.

  $\Rightarrow$ Recent molecular dynamics (MD) calculations have confirmed these distributions for low energy ions (Marion, 2006).

Chemically Sputtered Particles

- Molecules released from a surface through chemical reactions, eg., CH_4, WO_2, are generally considered to leave the surface with thermal energies, or near thermal energies.

- This will lead to sub-eV energies in most cases.

- Dissociation process, however, can lead to an increase in kinetic energy at some point in the neutral's lifetime, eg. Franck-Condon atoms.
  - Processes here are not very well known.

- Again, a cosine distribution is generally assumed for the released particles, however, surface potentials may lead to a more peaked distribution.

Impurities from the First Wall

- Most impurity atoms from the first wall are ionized in the plasma periphery before reaching the core plasma. This region is referred to as the Scrape-Off-Layer, or SOL, as there is a direct connection to a solid surface along the magnetic field lines.
- The most likely way for an impurity atom to enter the core plasma, is for it to be ionized inside the last closed flux surface.
- Here, we are not so interested in the effect of impurities on the core plasma, but on the manner in which impurities leave the core plasma.
- In steady state, the rate at which impurities enter the plasma will be equal to the rate at which they diffuse out of the core plasma into the scrape-off layer.

2.3 Plasma Transport: 1D SOL Model

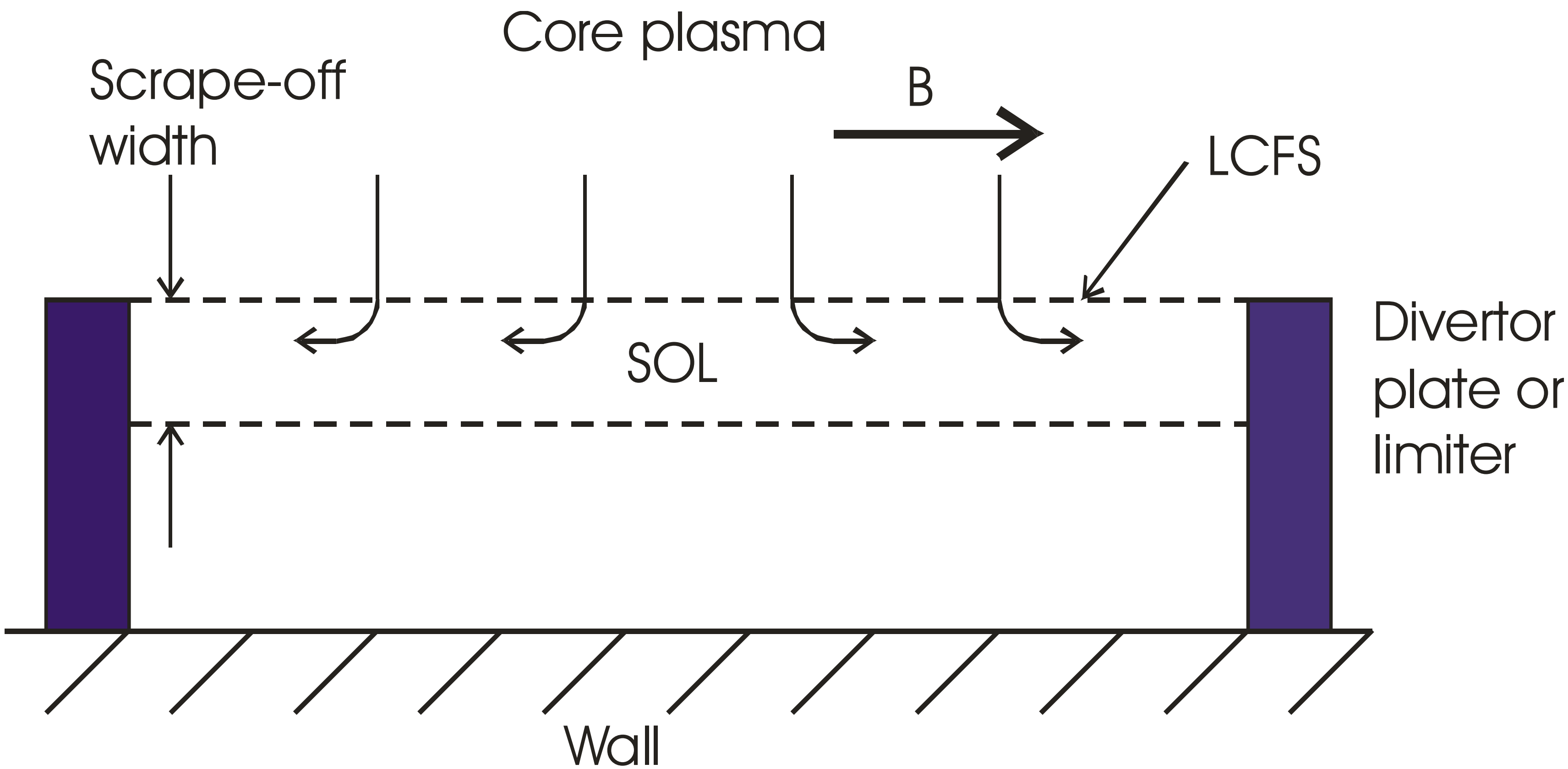

From Stangeby, 2000

- Transport across magnetic field lines is a slow diffusion process.
- However, once particles cross the LCFS into the SOL, there is rapid transport along the magnetic field lines to a solid surface.
- Due to the helical nature of the magnetic field, the connection length between two divertor plates can be 10's of meters.
- Thus there is some opportunity for cross-field diffusion to produce a scrape-off layer width of several cm.

$\Rightarrow$ This is important for power dissipation

- Essentially all impurity atoms which make it into the core plasma will eventually diffuse out to the SOL, and then be deposited on the divertor plates or other parts of the first wall.

- Similarly, impurity atoms/molecules which are ionized before entering the core plasma must be in the SOL, and thus will also largely end up on the divertor plates.

$\Rightarrow$ Most impurities originating at the first wall, which are not promptly redeposited as neutrals, will ultimately be deposited on or near the divertor plates.

$\Rightarrow$ This may, or may not be their final resting place!

Impurities from Divertor Plates or Divertor Region

- Looking at the 1-D SOL model again, the central region of the SOL collects energetic plasma particles which diffuse out of the core plasma across the LCFS.

- At the ends of the SOL, we have solid surfaces, which act as sinks for plasma particles.

- Thus, there is generally a strong flow of particles in the SOL, directed towards the divertor plates.

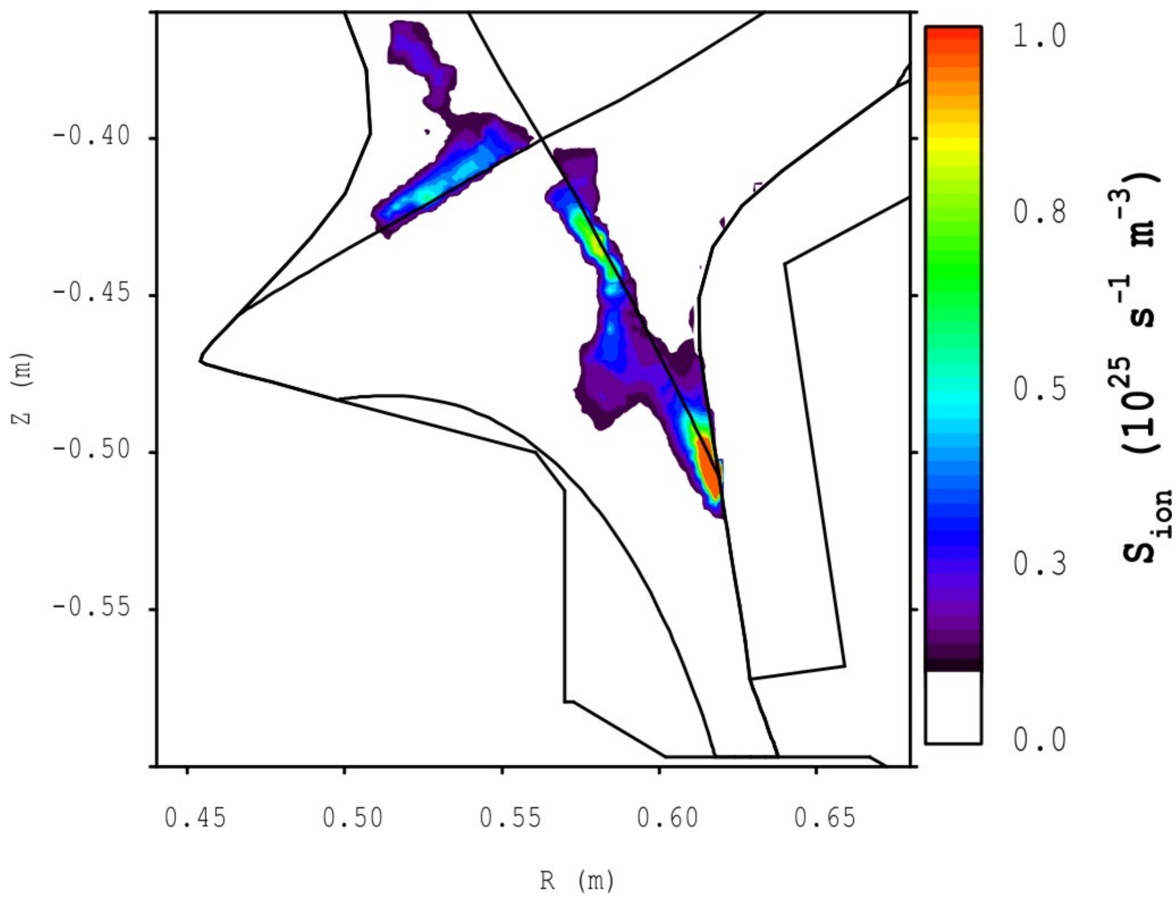

Figure: Hydrogen ionization rate in C-mod divertor (Lisgo, 2003)

- Impurities originating from surfaces in the divertor region are likely to be ionized in the SOL or private flux region.
- From there, they will quickly be recycled back to the divertor (due to the plasma flow towards the divertor plates).
- If the divertor is doing what it is intended to do, few impurities will make it inside the LCFS.

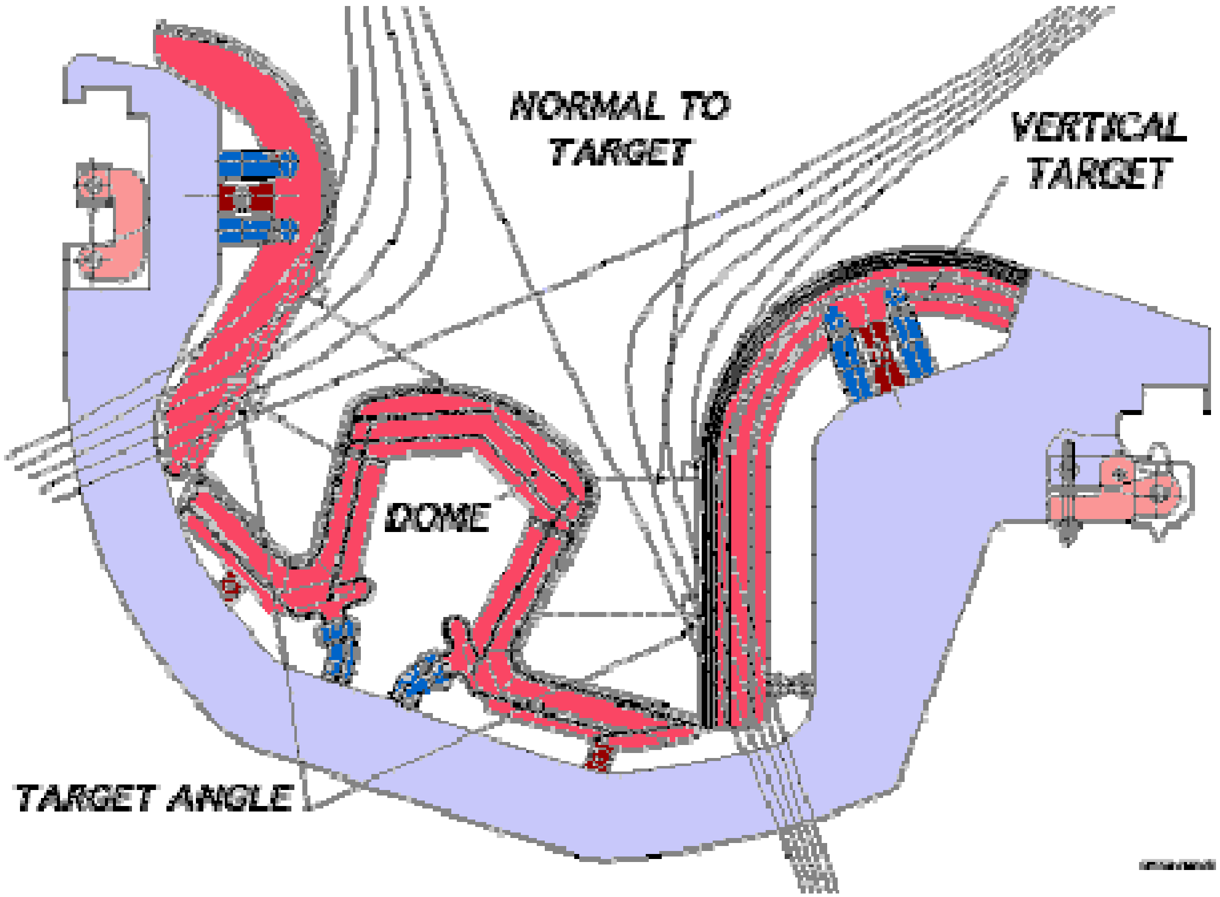

Figure: ITER divertor (www.iter.org)

- If the divertor plates are regions of net erosion, impurities will continue to be recycled until they go outside the region of ionizing plasma.
- If the divertor is net deposition, large thicknesses of deposits may build up very quickly.

Impurity Transport Conclusions

- We have nearly completed the impurity transport loop.
- In the last step, the impurities will be deposited on surfaces remote enough from the plasma so as not to receive significant ion or heat flux. this could involve:
  - re-erosion from the divertor plates
  - removal by some other event, eg., ELMS, disruptions.
- On those final locations, the impurities will continue to collect, until some form of outside removal process occurs.

2.4 Codeposition Patterns in JET

- In recent times, JET has operated with regular evaporation of Be on the first walls to reduce oxygen impurities.
- Thus, codeposited layers are a mixture of C and Be.
- The distribution of D (and therefore C?) and Be on two of the divertor tiles is shown in the figure.

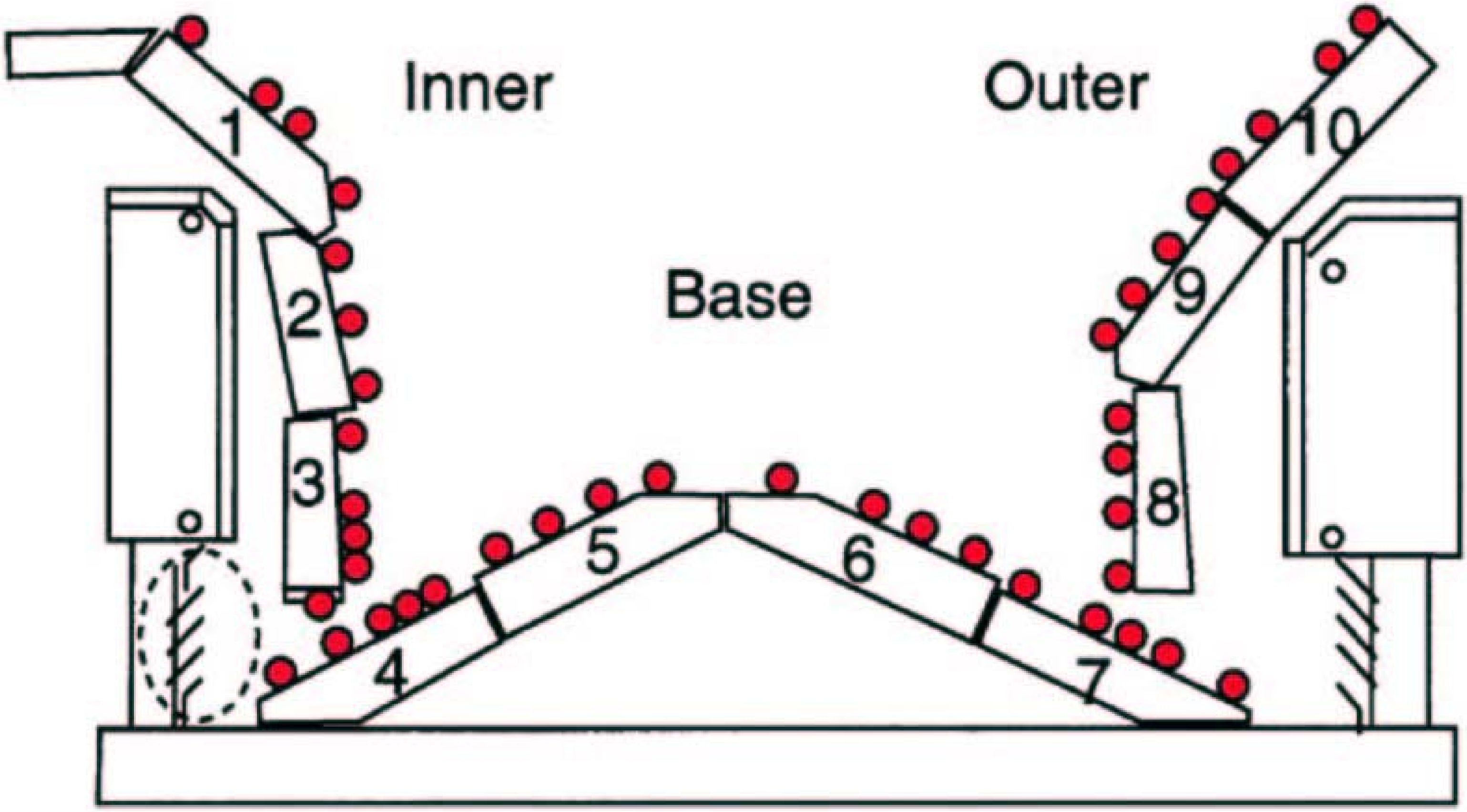

From Rubel, 2003

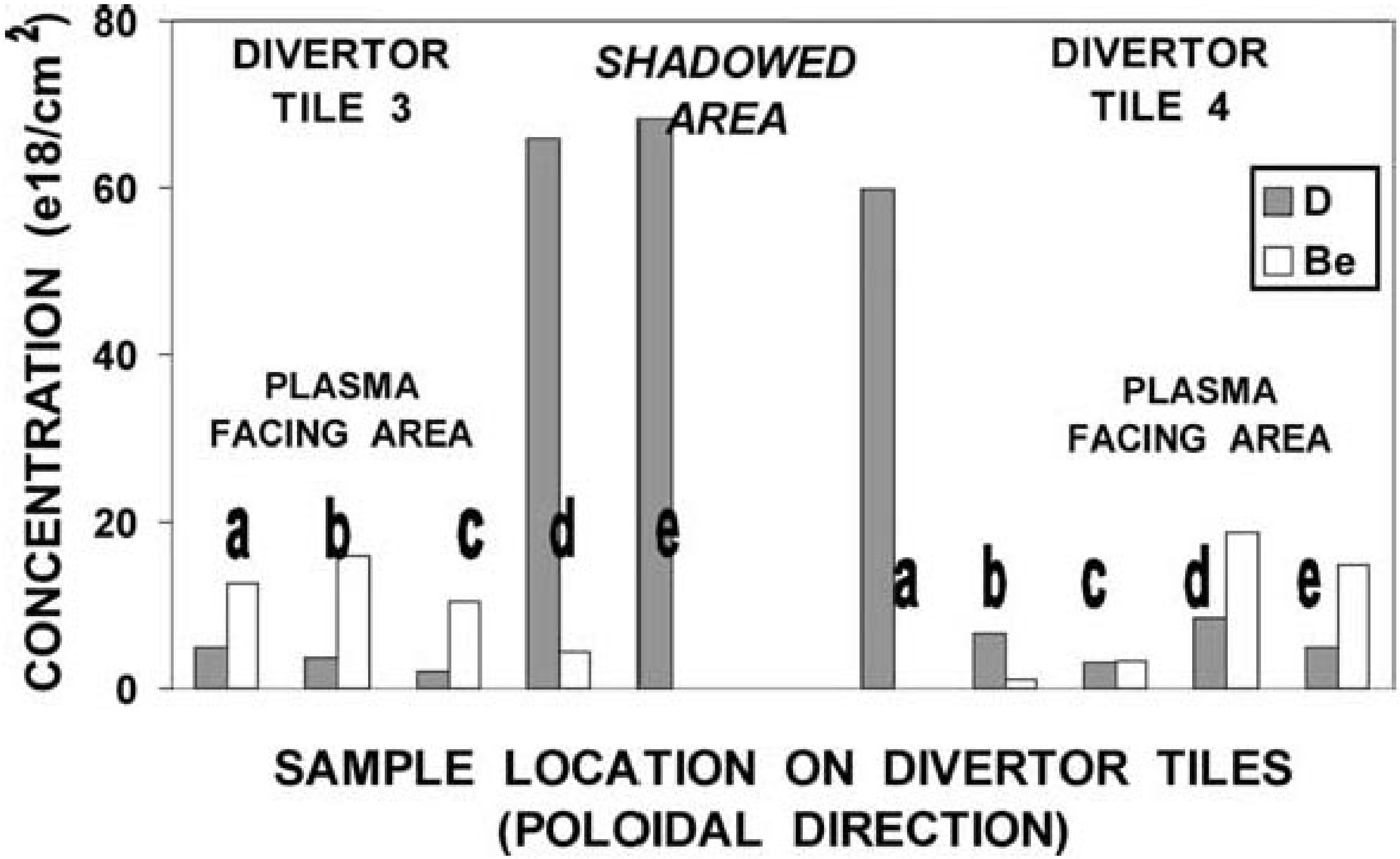

From Rubel, 2003

- Be appears to be deposited primarily on plasma-contact surfaces of the divertor plates.

- C is deposited primarily in shadowed regions, indicating the secondary transport of carbon.

- The louvers (circled) have also been shown to be important secondary carbon deposition locations.

$\Rightarrow$ Deposition patterns are very sensitive to the element involved, and also to the nature of the discharge.

2.5 Codeposition Patterns in DIII-D

- In the past couple of years, some specific experiments have been done to get a handle on this impurity transport issue.
- In order to separate out the deposit from the background ^{13}C is injected into the tokamak in the form of methane.
- Ion beam analysis of tiles removed from the tokamak is then used to determine the deposition pattern.

^{13}C injection in DIII-D

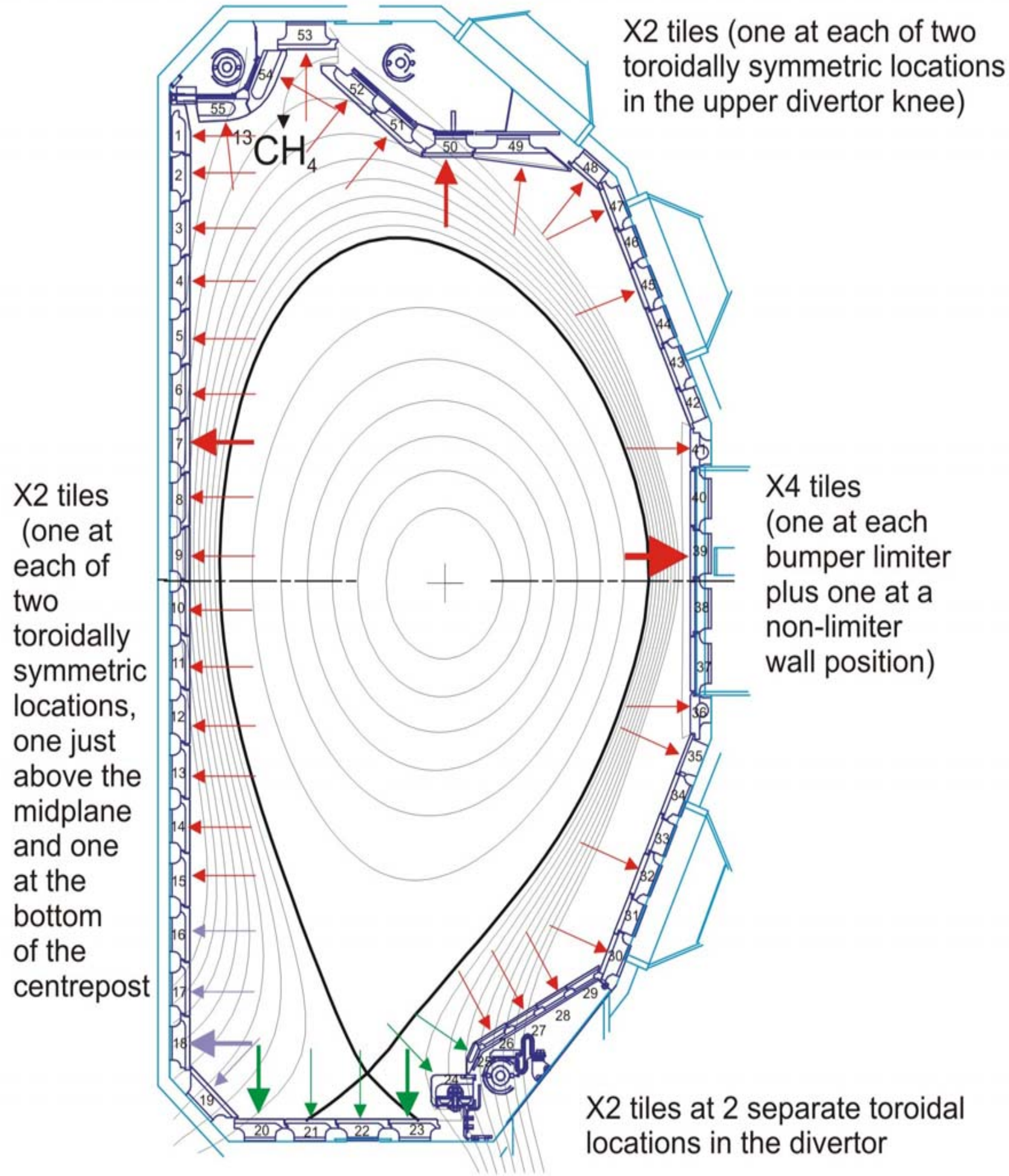

^{13}C deposition in DIII-D

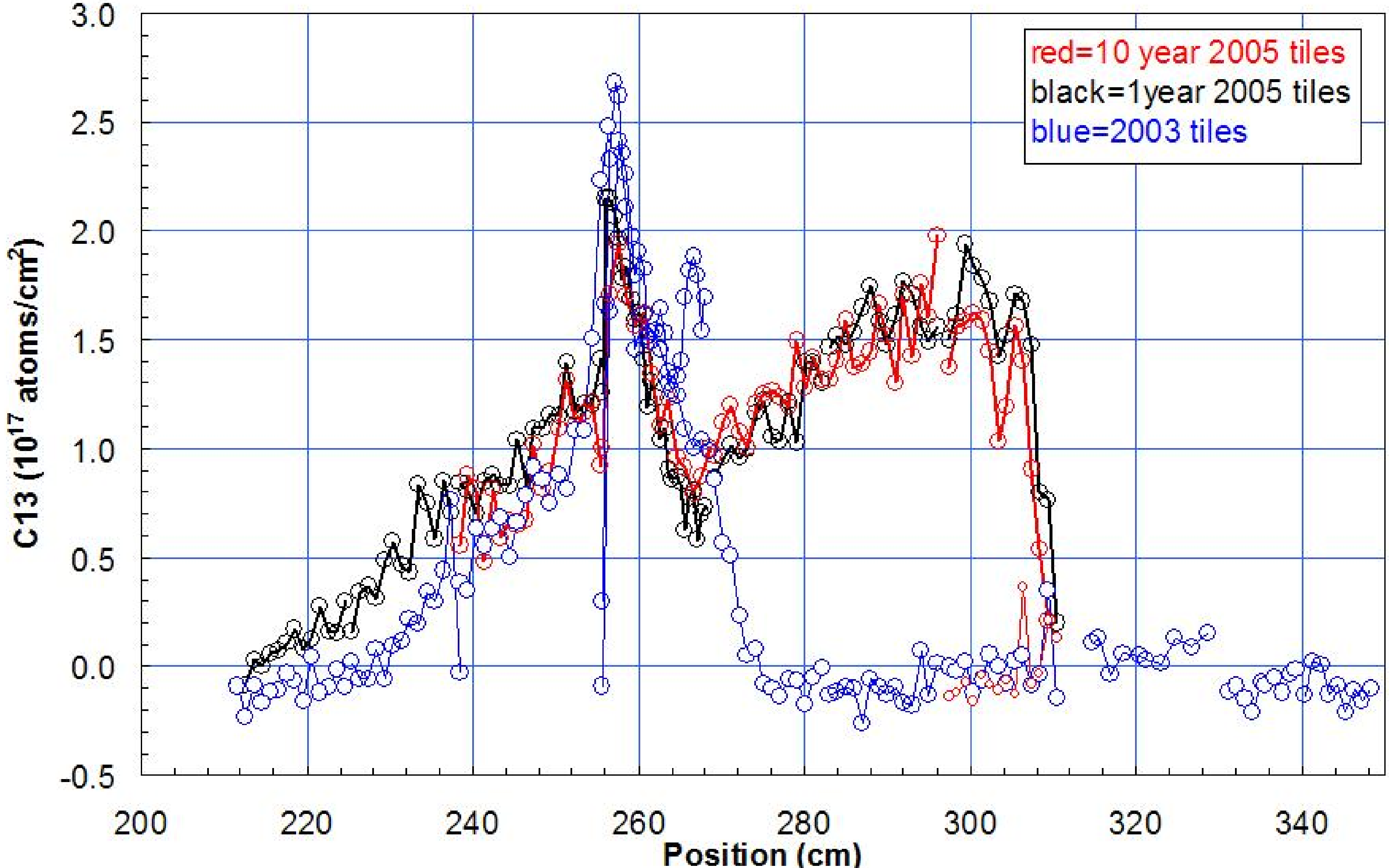

From Wampler, 2006

^{13}C deposition in DIII-D

- The largest deposition (~30% of injected ^{13}C) is in the inner divertor and private plasma regions.
- Lesser deposition was also found near where the gas was injected.
- Approximately half of the injected 13C remains unaccounted for, and it was not observed in the gasses pumped from the chamber. Our current thinking is that it has been deposited over a large region of the first wall in concentrations below the detection threshold.

3. Tokamak Film Characterization

3.1 Modified surface layers

3.2 Carbon films

3.3 Tokamak codeposits

3.4 Codeposition with beryllium

3.5 Codeposition with Tungsten

3. Tokamak Film Characterization

- There are many ways of depositing films, several of which may be operating in a tokamak at any given time.

- Here, I will focus on carbon films, as this is currently the concern in ITER and current tokamaks.

- There is also a bit of information on Be and W codeposited films which we will look at, in the last part of this section.

  $\Rightarrow$ In a tokamak with several materials interacting with the plasma (eg., ITER), codeposits will have a varying and unpredictable composition.

3.1 Modified Surface Layers

- All plasma-facing surfaces in a tokamak will be immediately modified upon exposure to the plasma.

- The flux of energetic particles leads to two results:

  1) Surfaces are saturated with hydrogen, in carbon: H/C ~ 0.4 (at ~300 K).

  2) Sputtering/erosion of the surfaces leads to changes in surface morphology.

     $\Rightarrow$ blistering in metals (figure)

- In some ways, at least in carbon, the implant layer is similar to plasma-deposited films.

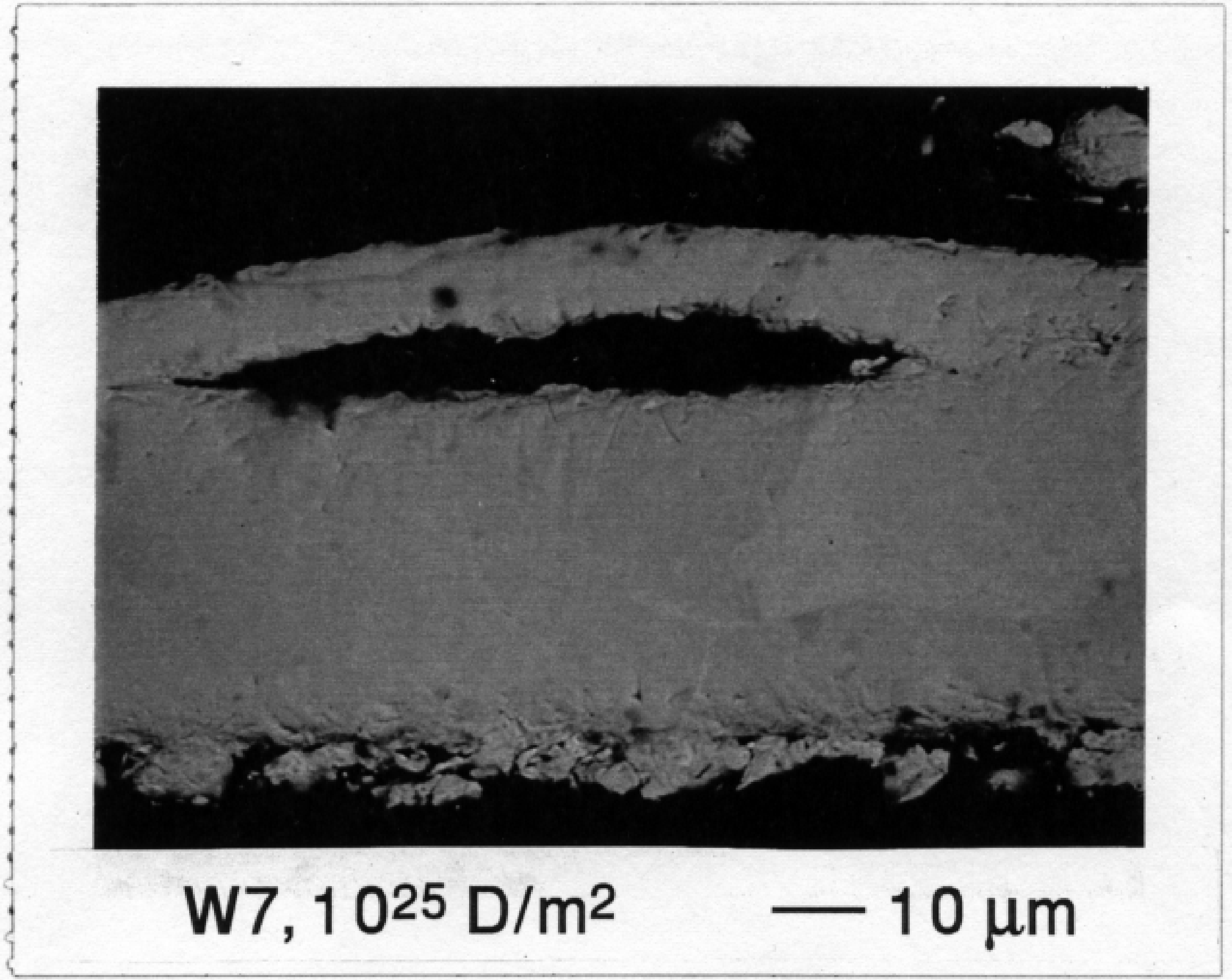

From Haasz, 1999

3.2 Carbon Films

- While there is a broad spectrum of carbon-based films, they are generally categorized as one of two types (eg., Jacob, 1998):

    1) Hard films
    2) Soft films

- Hard films are generally of higher density, and have lower hydrogen content. If the bond structure is primarily sp^3 (similar to those found in diamond), such films may be referred to as diamond-like.

- Soft films have lower density and higher hydrogen content, with many of the carbon atoms bonded to hydrogen atoms. Often referred to as polymer-like due to the hydrocarbon polymers.

- It is also possible to produce diamond films (deposition at 800 – 1000 K).

Hard Carbon Films

- Primary production indicator is the higher energy of the incident carbon/hydrogen ions.
- Hard films generally have a lower hydrogen content, and thus more carbon-carbon bonding, resulting in stronger films.
- Typical densities 1.2 - 1.6 g/cm^3.
- Hydrogen content < 0.4 H/C.
- Such films have good adhesion to many types of substrates, and have many practical applications, such as protective coatings.

Soft Carbon Films

- Lower bombarding energies of the incident species allows hydrocarbon polymers to survive.
- Deposition in the presence of a large flux of hydrogen, at temperatures low enough that the hydrogen is not desorbed.
- Typical densities ~ 1.2 g/cm^3
- H/C ratios ~ 1
- Films tend to have large differences in thermal properties compared to graphite. They also absorb moisture on exposure to air, resulting in large scale flaking.

3.3 Tokamak Codeposits

- In soft films, the H/C ratio ~ 1 means that every carbon atom deposited takes a hydrogen atom with it.

  $\Rightarrow$ tend to form on non-plasma facing surfaces with lower particle energies.

- Hard films tend to form in regions of more energetic plasma exposure.

  $\Rightarrow$ deposition in tokamaks can cover a wide range of film types.

- Even in "all-carbon" tokamaks, there are always some metal components, Also, some elements, such as boron, are deliberately deposited on wall surfaces. Thus films will be complicated due to the inclusion of these impurities.

Analysis of Codeposits in TFTR

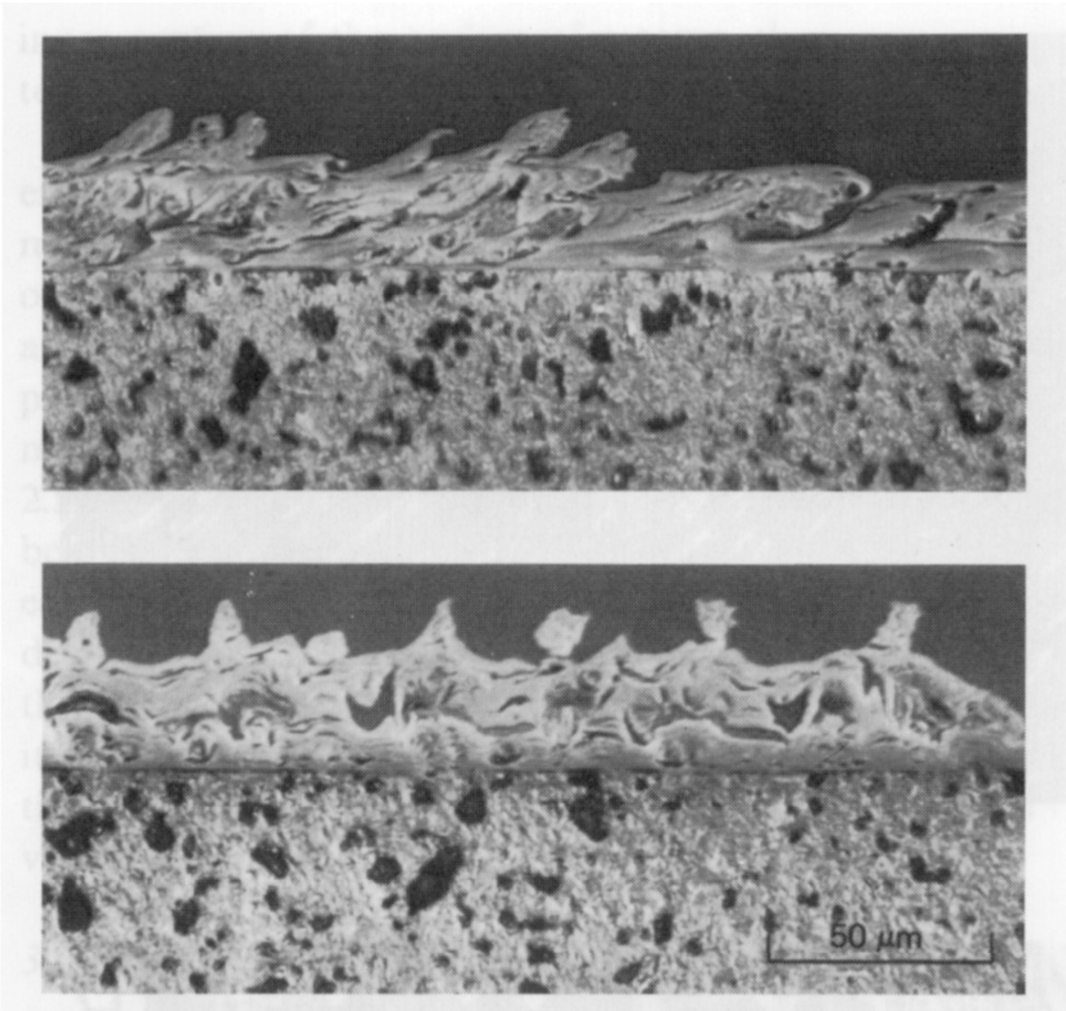

- Tile cross-sections from a region of “moderate” deposition.

- Primary impurities were Ni, Fe, Cr. Concentrations varied through the deposit, with maximum concentrations of ~ 1.5 at%.

From Mills, 1989

Analysis of Codeposits in DIII-D

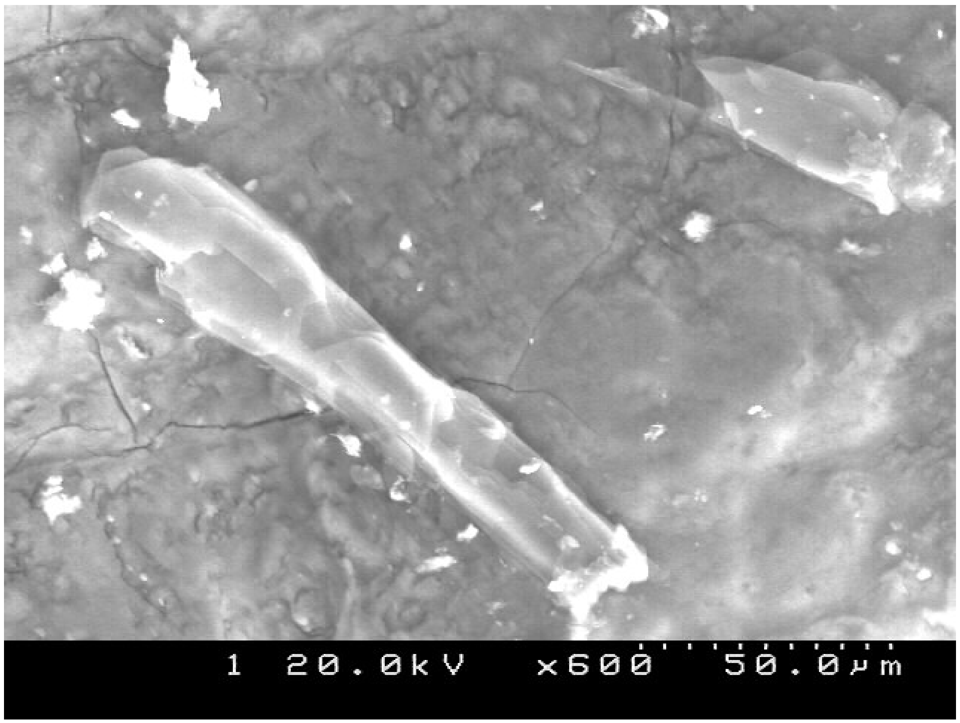

- Deposits in DIII-D generally have a large concentration of boron, due to boronizations.
- > 50% B at midplane.
- ~ 10% B on upper divertor.
- Balance of deposition carbon.
- Photo show boric acid crystal from upper divertor, from Wright, 2003.

Analysis of Codeposits in JET

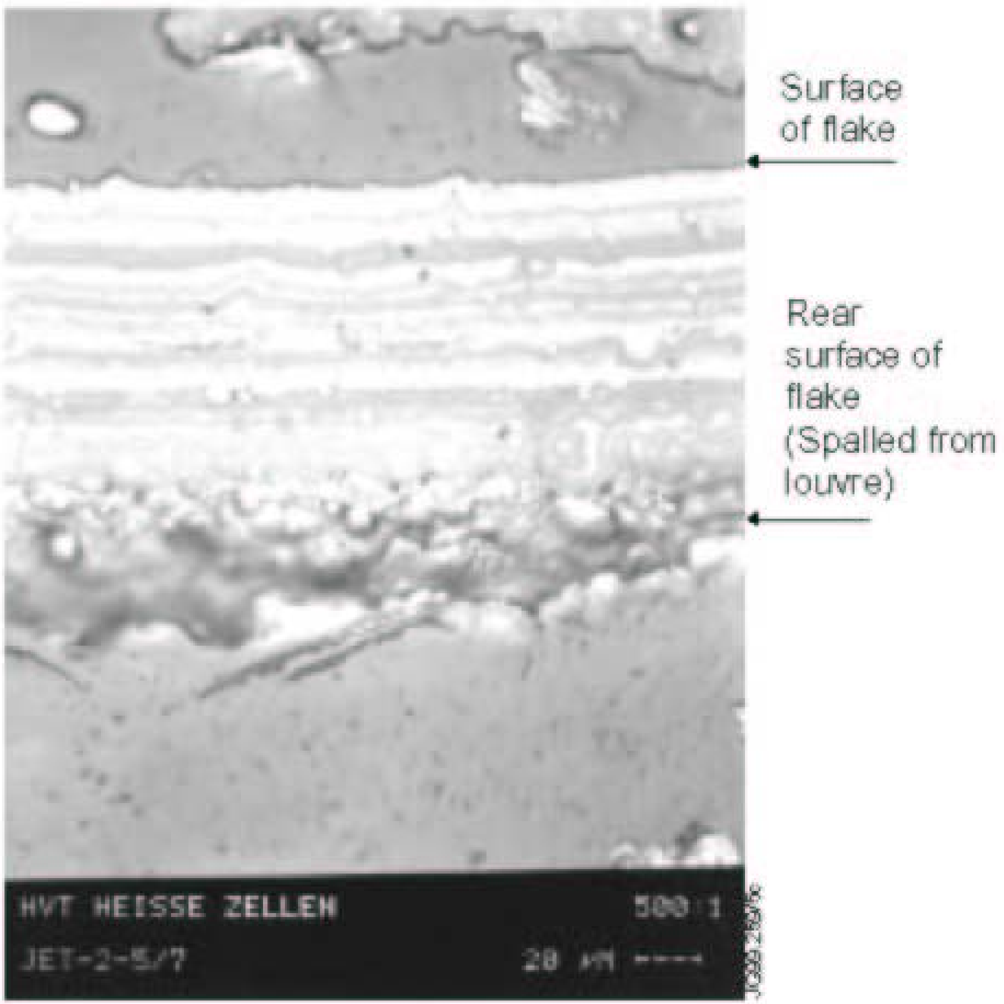

- Cross-section of a flake from the JET divertor.
- Thickness ~ 100 μm
- From Federici, 2001

Analysis of Codeposits for TEXTOR

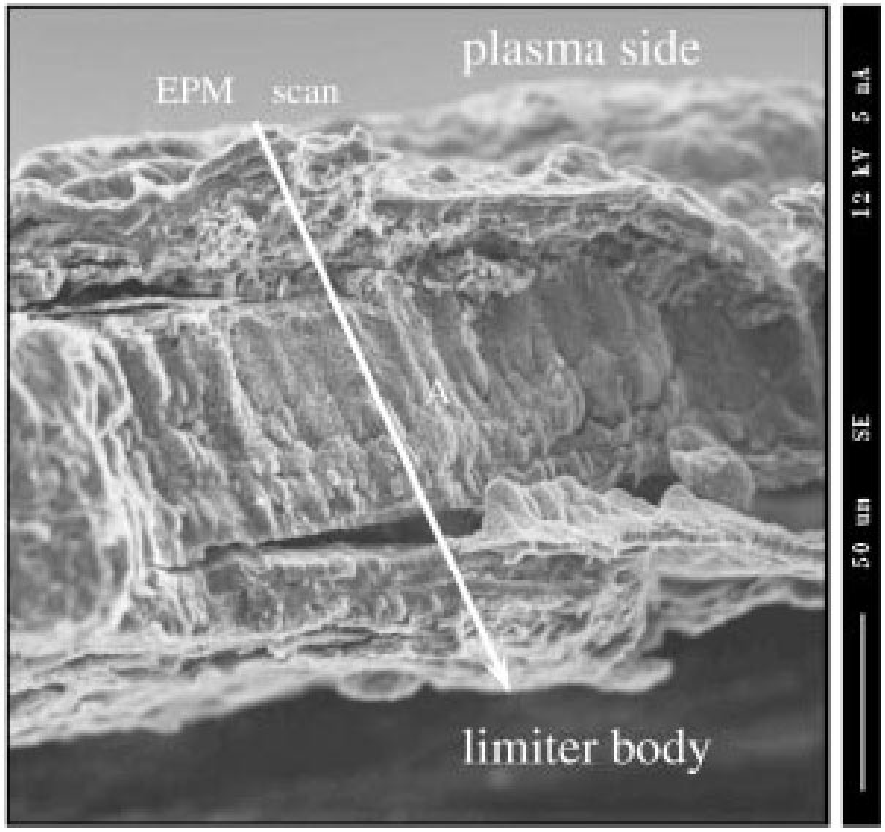

- Flake from the side of the TEXTOR limiter; flakes as thick as 170 μm, and as large as 10 mm were observed.

- From von Seggern, 1999

3.4 Codeposition with Beryllium

- Since there are no tokamaks operating with all Be plasma-facing surfaces, we must look to laboratory measurements.

- The solubility of hydrogen in Be is very low, and codeposition with pure Be is not likely to be significant.

- The hydrogen concentration in Be-based codeposits with oxygen or carbon impurities may be similar to carbon codeposits.:

  $\Rightarrow$ Figure

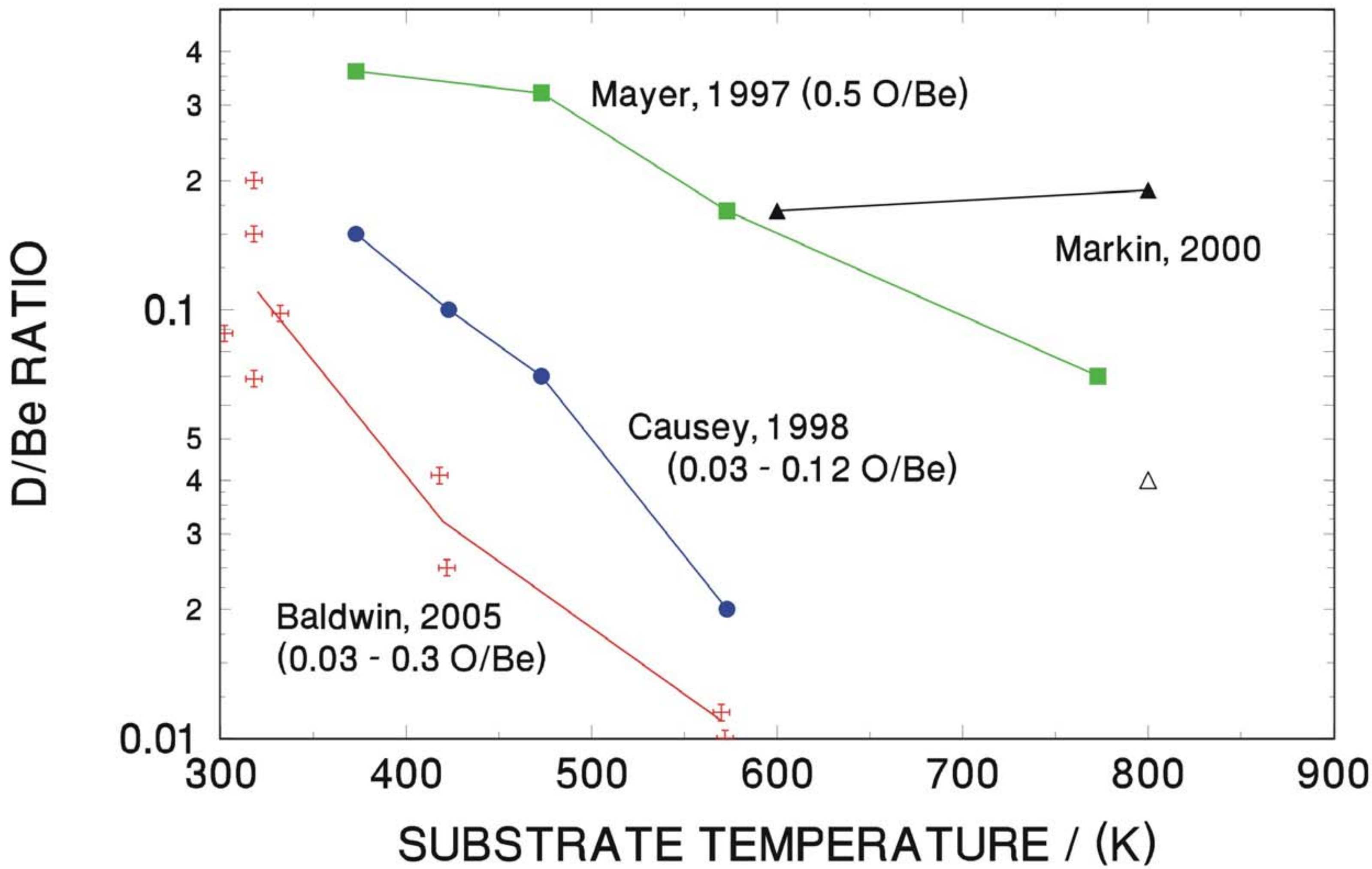

J. W. Davis, IAEA Workshop on Atomic and Molecular Data for Fusion Energy Research, August 28 - September 8, 2006, International Centre for Theoretical Physics, Trieste

- The rate of codeposition may be more closely related to the flux of oxygen and carbon than to the flux of Be.

- This makes predictions more difficult.

3.5 Codeposition with Tungsten

- ASDEX-U tokamak is now largely W walls, plasma-sprayed W on graphite tiles.

- Future analysis of codeposits may give us some information about the effect of W on codeposition.

- Current codeposits now largely carbon, with a small W content.

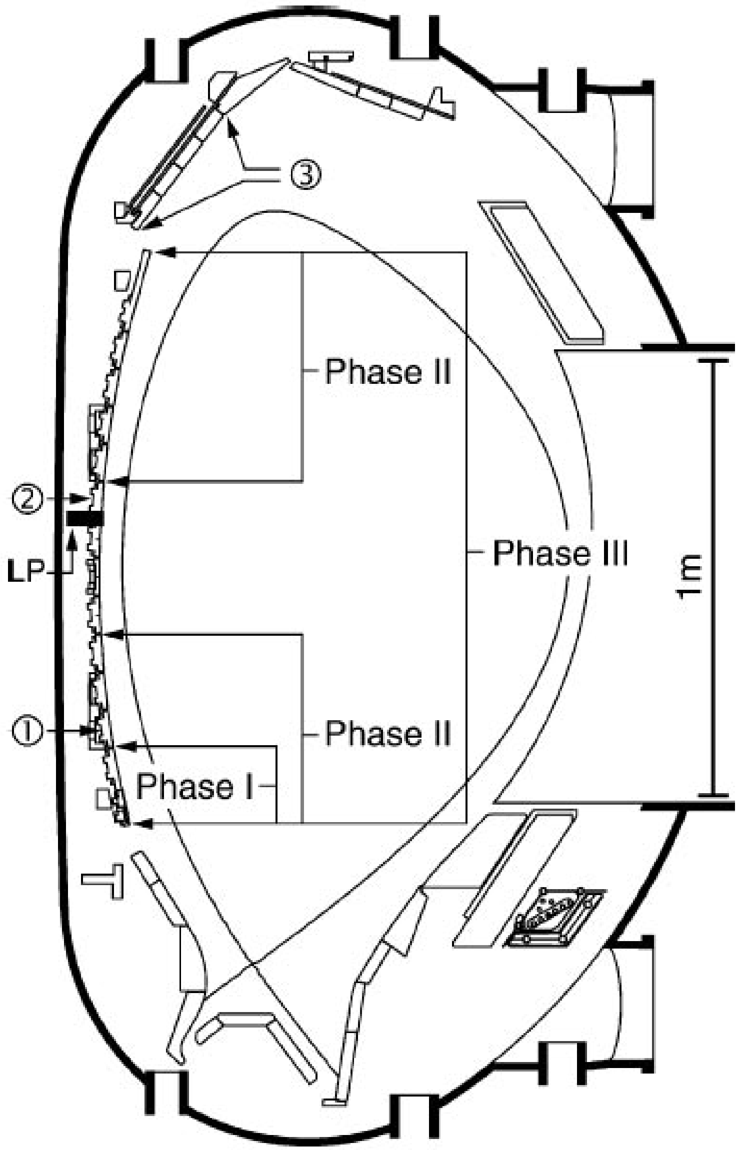

- W deposition now found in areas surrounding the divertor targets.

From Krieger, 2003

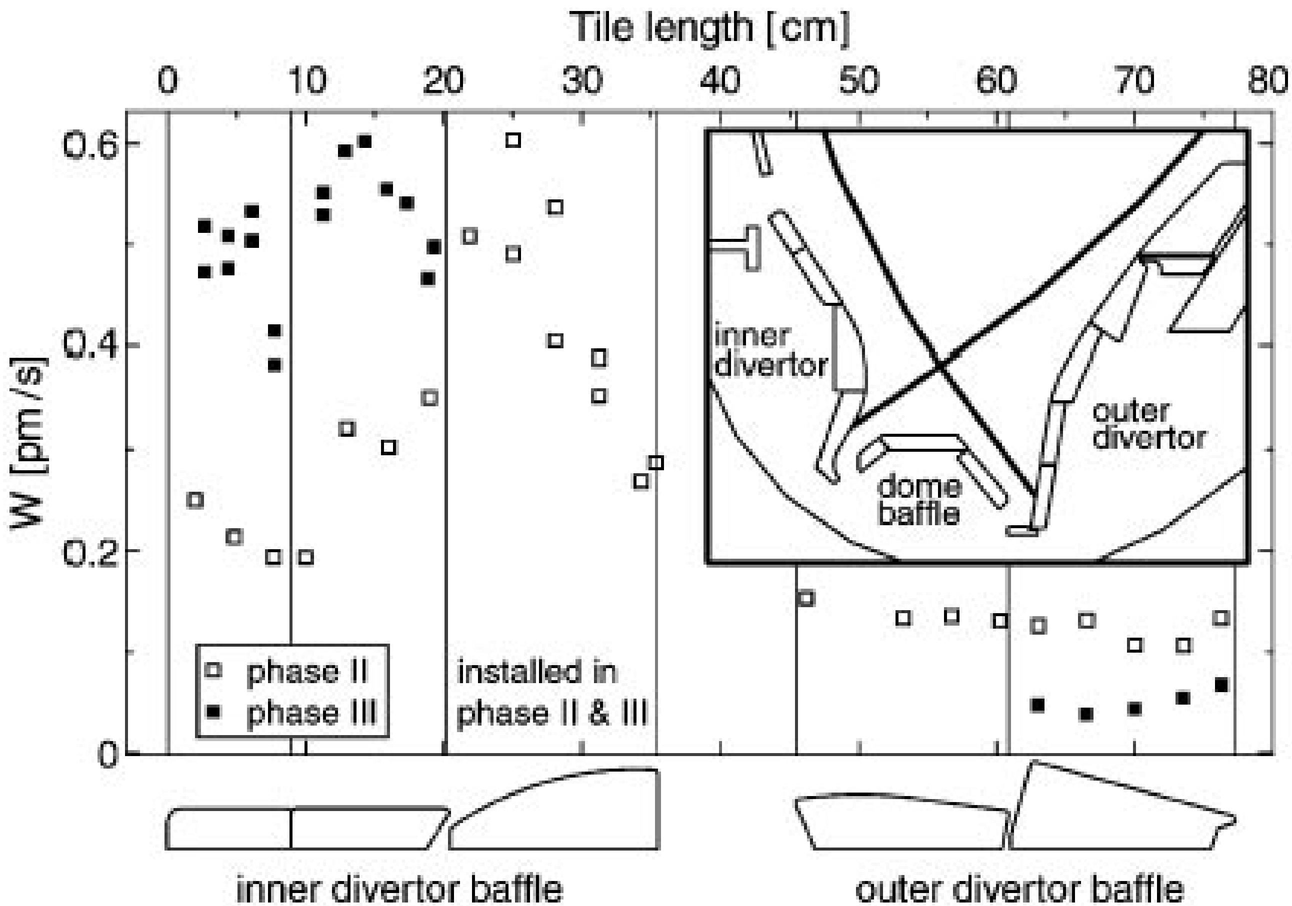

From Krieger, 2003

4. Plasma Interactions with Codeposits and Mixed Materials

4.1 Erosion of a-C:H films

4.2 Erosion of bulk mixed materials

4.3 Modified/mixed surfaces

4. Plasma Interactions with Codeposits and Mixed Materials

- Carbon-based codeposited films have been studied in the laboratory setting for more than 20 years.

- Typically, such films are easier to erode than pure graphite, but erosion rates depend strongly on the nature of the film.

- Films deposited in tokamaks, however, will be more complicated than laboratory-produced films, because of the inclusion of other elements.

  $\Rightarrow$ Such as B due to boronization.

- In ITER, deposits will likely be a complex mixture of Be, C, W and H.

  $\Rightarrow$ There is no experience with such films.

4.1 Erosion of a-C:H films

- Energetic (> 100 eV) H^+ bombardment of graphite leads to the formation of a near-amorphous hydrogenated layer, which is similar to a-C:H films.

  $\Rightarrow$ Ion erosion of films similar to erosion of graphite.

- Low energy H^+/H° erosion of a-C:H films occurs at rates comparable to more energetic H^+.

  $\Rightarrow$ The amorphous nature of the films make up for the lack of ion-induced damage.

  $\Rightarrow$ Figure

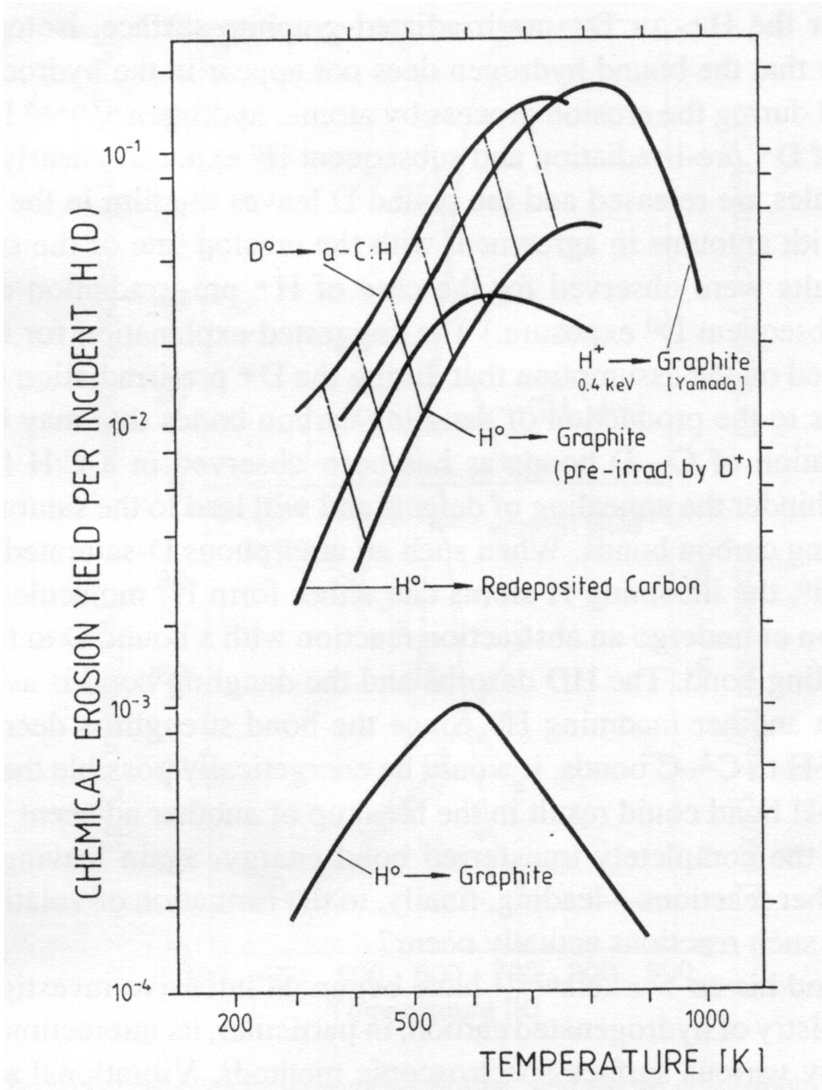

From Vietzke, 1996

- In regions which have large fluxes of low energy H^+ and $H°$, deposited carbon films are quickly removed through chemical erosion.

- There can also be a thermal decomposition of the films, leading to the release of hydrogen or hydrocarbon radicals (von Keudell, 1999).

  $\Rightarrow$ Films can only survive in regions where there is the right balance of hydrogen and carbon fluxes, and also the right temperature range.

- This ease of removing deposited films may lead to the secondary transport of carbon from the divertor region to the surrounding surfaces.

- Films containing impurities may have substantially different erosion properties.

4.2 Erosion of Bulk Mixed Materials

- A number of studies have been carried out on the erosion of mixed materials in a fusion context.

- None is an exact model of what might happen in ITER, but they give us some Ideas of what may happen.

- There are two types of mixed materials which may arise in a fusion setting:

    $\Rightarrow$ Bulk mixtures or alloys (eg., doped graphites)

    $\Rightarrow$ Mixed surfaces created by impurities in the plasma.

Erosion of doped Graphite

- One of the most studied mixed material systems are doped graphites.

- The objectives have been to reduce the chemical activity (hydrocarbon formation) of carbon through the inclusion of less reactive elements.

- Various dopants include: B, Si, Ti, Va, W, etc.

- Such materials generally exhibit reduced erosion as compared to pure graphite, particularly for higher energies and higher temperatures.

$\Rightarrow$ Figure (Garcia-Rosales, 1992)

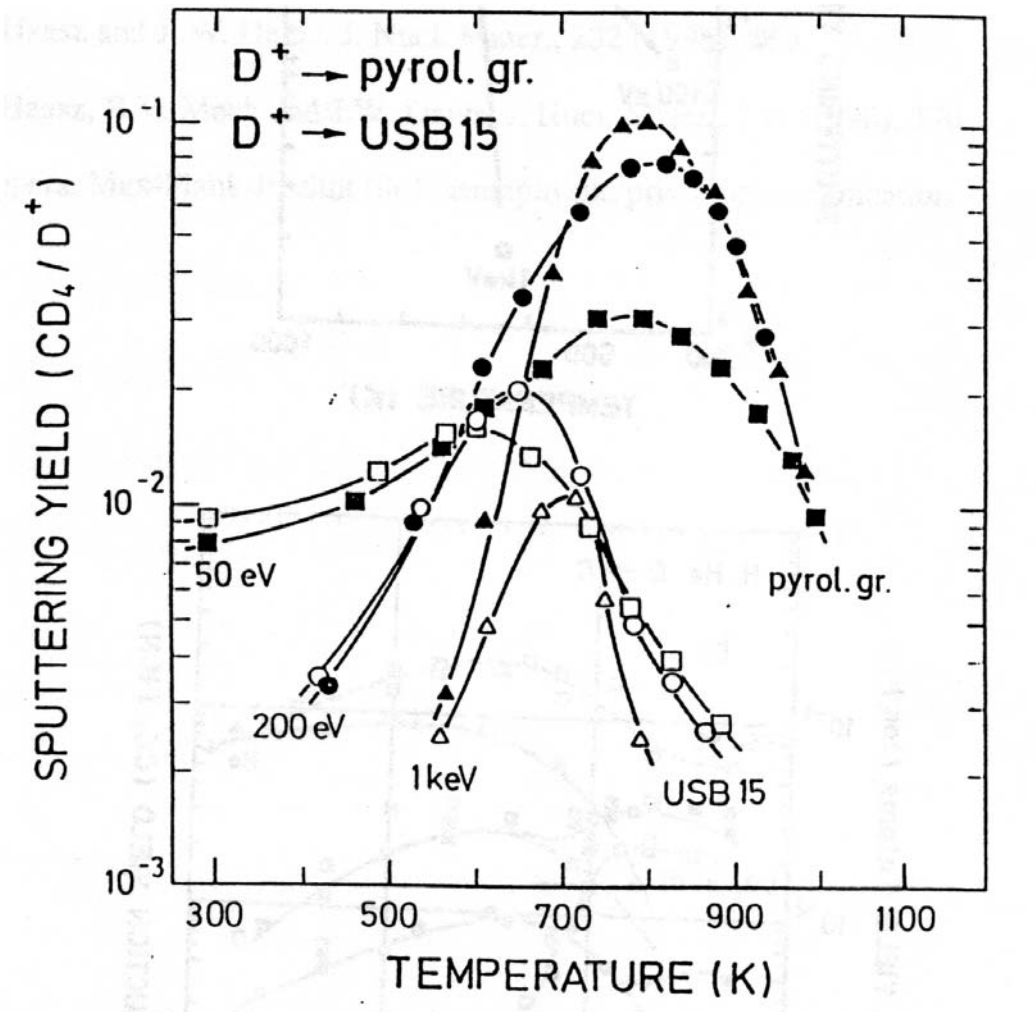

From Garcia-Rosales, 1992

- For lower ion energies, erosion yield reductions are comparable to the fraction of impurities.

$\Rightarrow$ Figure

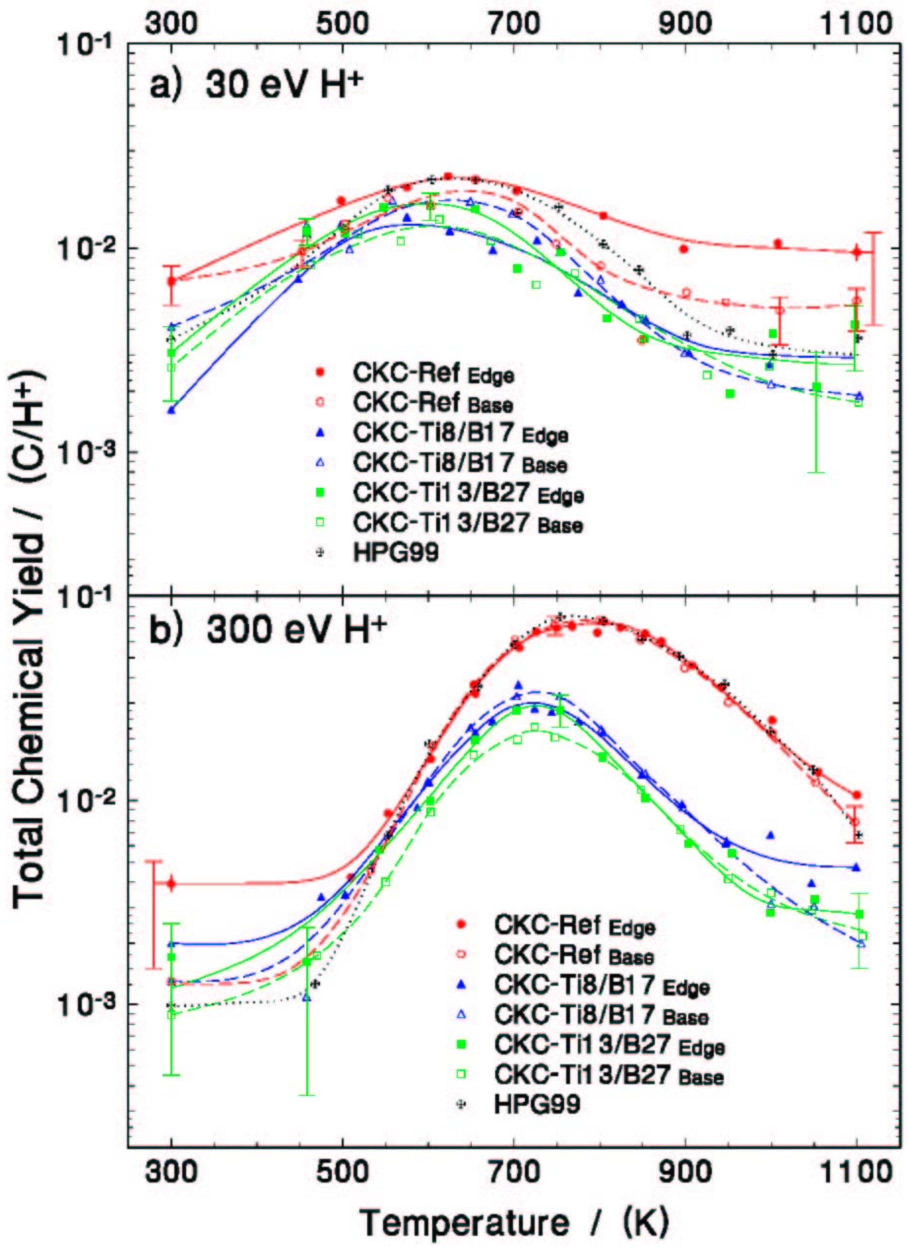

It is not clear that doped graphites would have a significant advantage in a tokamak

From Davis, 1998

4.3 Modified Surfaces

- In the laboratory, modified surfaces can be created through bombardment with almost any species.

- In the following slides, we will have a look at a number of fusion relevant systems, where a modified surface has been created and in some cases subjected to a simultaneous or sequential hydrogen flux.

The Carbon/Tungsten System

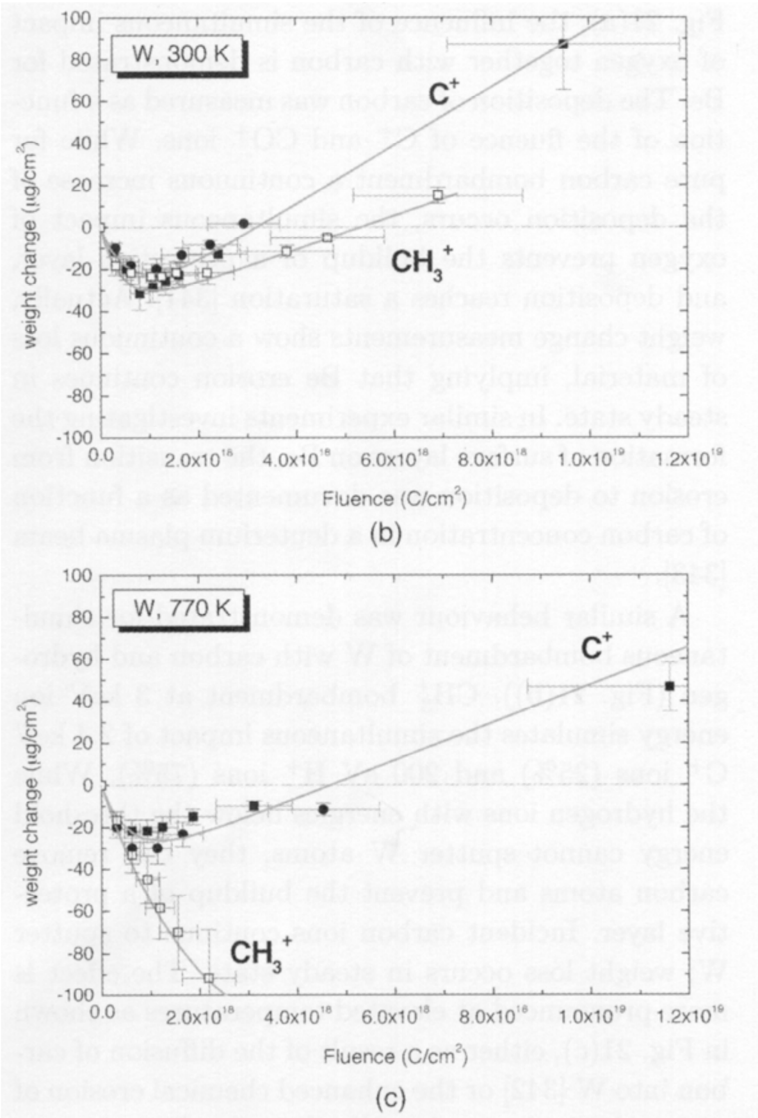

- Experiment has been carried out by using either C^+ or CH_3^+ ion beams on a W target.
- Initially there is mass loss due to sputtering.
- Eventually, the W becomes covered with enough C that sputtering of W stops.
- At the higher temperature, the erosion (or diffusion) of C reduces effect.
- Figure Krieger, 2001

The Carbon/Beryllium System

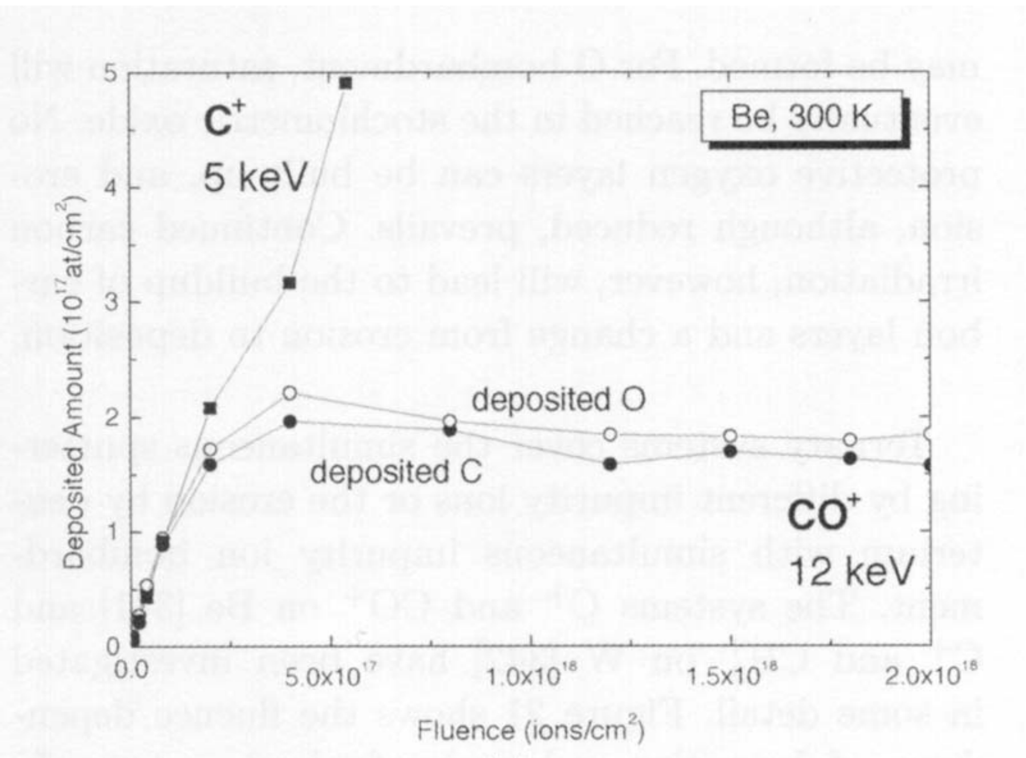

- A similar study has been carried out for C^+ and CO^+ bombardment of Be.
- Without the oxygen component, there is a rapid build-up of C on the surface.
- Adding the oxygen component leads to a balance between deposition and erosion.
- Figure: Goldstrass, 1999

The Beryllium/Carbon System

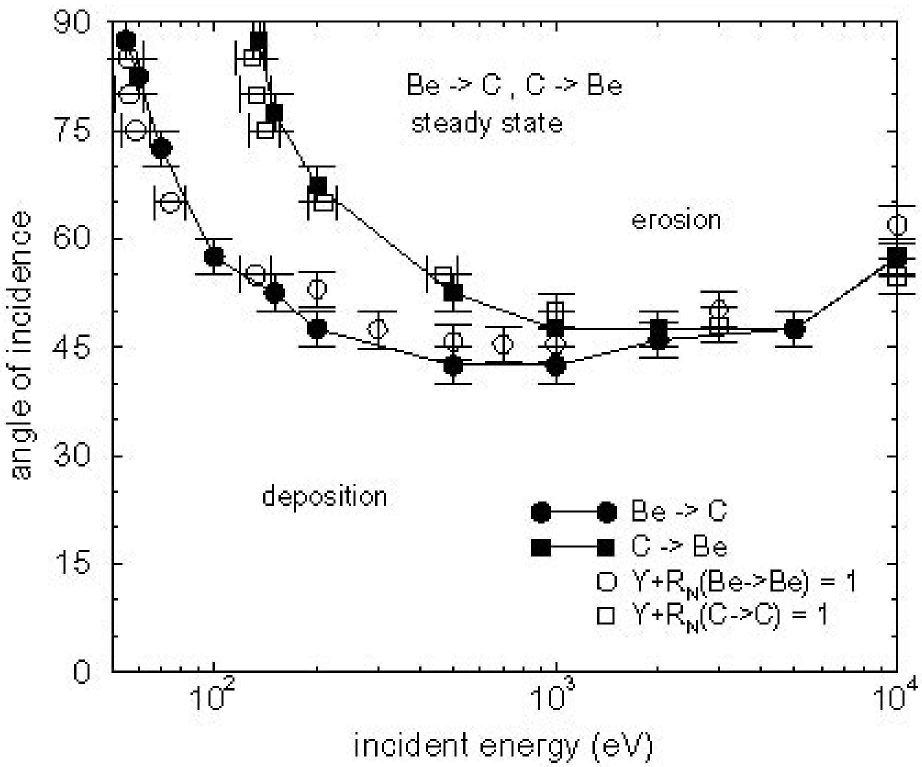

- Similar to the previous experiments, but calculations of Be incident on C and C incident on Be.
- In both cases, the system is deposition dominated.
- However, in a tokamak, there will be a hydrogen flux 100 times larger.

Figure: Eckstein, 2000

Hydrogen Retention in Carbon-Implanted Tungsten

- The hydrogen retention properties of a material may be changed substantially due to the inclusion of impurity elements.

- We will have a look at the C/W/H system, where we looked at the retention of hydrogen in a tungsten foil following C^+ bombardment.

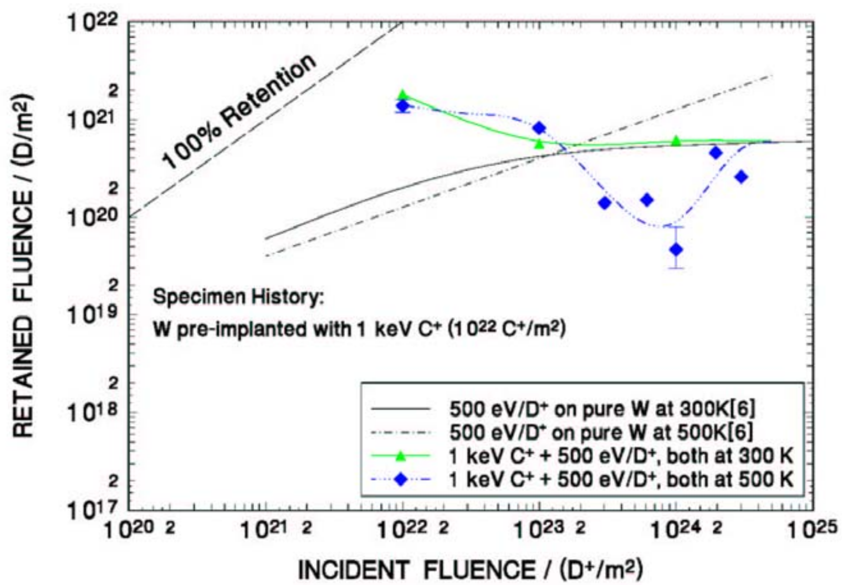

Figure: Poon, 2000

- Three retention regimes observed:

1) Retention in pure carbon
2) Retention in tungsten carbide
3) Retention in pure tungsten.

- Depending on the relative C^+ and H^+ fluxes to a W surface, any, or all of these situations might exist in a reactor.

Ongoing Experiments

- Plasma bombardment of carbon by a deuterium plasma with Be impurities (PISCES).

  $\Rightarrow$ Under what conditions does a Be layer accumulate?

- Atomically dispersed doped carbon films (Garching).

  $\Rightarrow$ How does a small W impurity affect erosion?

- Deposition rates in tokamaks (JET, ASDEX-U, DIII-D, etc.).

  $\Rightarrow$ Relating plasma conditions to the location of deposition.

Summary

- The existence and nature of films deposited in tokamaks will depend greatly on the exact bombardment conditions.

  ⇒ In particular, the impurity content of the plasma and the erosion conditions at deposition surfaces.

- Erosion yields, and hydrogen retention properties can vary by orders of magnitude.

- It is a great challenge (impossible!) to make predictions for a machine like ITER.

5. Removal of Codeposited Films

5.1 T removal from JET and TFTR

5.2 Removal of codeposited films by oxidation

5.3 Surface heating techniques

5.4 Mechanical scrubbing

5. Removal of Codeposited Films

- Three general types of procedures have been proposed for codeposit removal in ITER, and tokamaks in general.

  $\Rightarrow$ Oxidation (thermal, plasma)

  $\Rightarrow$ Surface Heating, either large scale or local (eg., laser ablation)

  $\Rightarrow$ Mechanical scrubbing (eg., water jets)

- Our first step will be to look at the experience in JET and TFTR.

5.1 T Removal in JET and TFTR

- Tritium has been used on a large scale in both JET during the DTE1 runs in 1997, and in TFTR between 1993 and 1997.

- In JET, a total of 35 g of T was introduced into the torus. At the end of the experiments, 11.5 g, or ~ 33% remained in the torus.

- In TFTR, 5.2 g of T was introduced into the torus, with 2.6 g, or ~ 50%, remaining in the torus.

- Various techniques were then applied to the machines to reduce this retained amount.

Tritium Removal from JET 1

Procedure	Comments
Deuterium tokamak pulses	> 1000 shots reduced the in-vessel inventory by a factor of 2, 11.5 to 6 g.
ICRF heated discharges	More effective than ohmic discharges; wall inventory reduced from 4.4 to ~ 2.9 g (partway through campaign).
He glow discharge cleaning	Ineffective
D glow discharge cleaning	Ineffective, required a large amount of gas processing
D_2 gas soaks	Ineffective
Outgassing	Ineffective

Tritium Removal from JET 2

Procedure	Comments
ECRH conditioning plasmas	Ineffective
N_2 vents	Ineffective
Baking divertor surfaces	Heating divertor structure from 310 to 410 K released a small amount of T (6 mg).
Vessel venting to air	2 g of T released in 4 months of air ventilation of torus.
Remote tile exchange	Divertor tiles, flakes, etc., physically containing ~ 0.6 g T.
Bakeout of vessel	Bakeout in 1999 released further 1.25 g.

Source: Andrew, 1999

Tritium Removal from TFTR 1

Procedure	Comments
Deuterium tokamak pulses	Ineffective
He glow discharge cleaning	Ineffective
D glow discharge cleaning	Initially high removal rate.
D_2 gas soaks	Ineffective
Outgassing	Ineffective
He/O glow discharge cleaning	Rate ~ 5 mg/hour, constant with time.

Tritium Removal from TFTR 2

Procedure	Comments
Disruptions	14 mg recovered after one major disruption
Pulsed discharge cleaning	Heats limiters to ~ 520 K; 100 mg T removed over 23 hours
Boronization	Little T released, most near surface tritium previously removed
Vessel venting to air	220 mg T released in 1 hour exposure to air, considered most effective technique.

Source: Federici, 2001

T Removal from JET and TFTR: Summary

- The long-term T retention in JET was 2.1 g T, or ~ 6%.
- The long-term retention in TFTR was 0.6 g T, or ~ 12%.

  ⇒ These values are at about 2 orders of magnitude higher than acceptable in ITER or a future fusion reactor.

5.2 Removal of Codeposited Films by Oxidation

- Oxidative procedures apply primarily to carbon-based codeposits. They would not likely be effective on Be or W-based codeposits.

- Oxidative methods fall into 3 general categories:

  1) Thermal oxidation

  2) Plasma-driven oxidation

  3) Ozone

5.2.1 Thermal Oxidation

Procedure

- Film surfaces are heated moderately in the presence of O_2, and the film is essentially burned off.

Thermal Oxidation: Advantages

- The technique is not restricted by the magnetic field. Field coils would not have to be turned off.
- Can reach all areas inside the tokamak, including between tiles and in pumping ducts where codeposits are known to form.
- Effects can be localized through selective heating of various regions in the tokamak.
- The method is supported by a fair body of laboratory research.
- Minimal effect on other reactor components.

Thermal Oxidation: Disadvantages

- Requires oxygen in the machine. This may be highly undesirable, as some surfaces (eg., Be walls) may absorb the oxygen, and reemit it into the plasma during discharges, leading to high plasma impurity levels, and subsequently higher erosion yields.
- Process is slow at low temperatures. May be too slow at temperatures achievable in ITER.
- Ineffective at removing films containing common impurities such as boron (Davis, 2001a).

Thermal Oxidation: Lab Results 1

- Several key results have been demonstrated in the laboratory:

1) The release of hydrogen during O_2 exposure is due to chemical reactions between the oxygen and the carbon component of the film.

$\Rightarrow$ Figure (Wang, 1997)

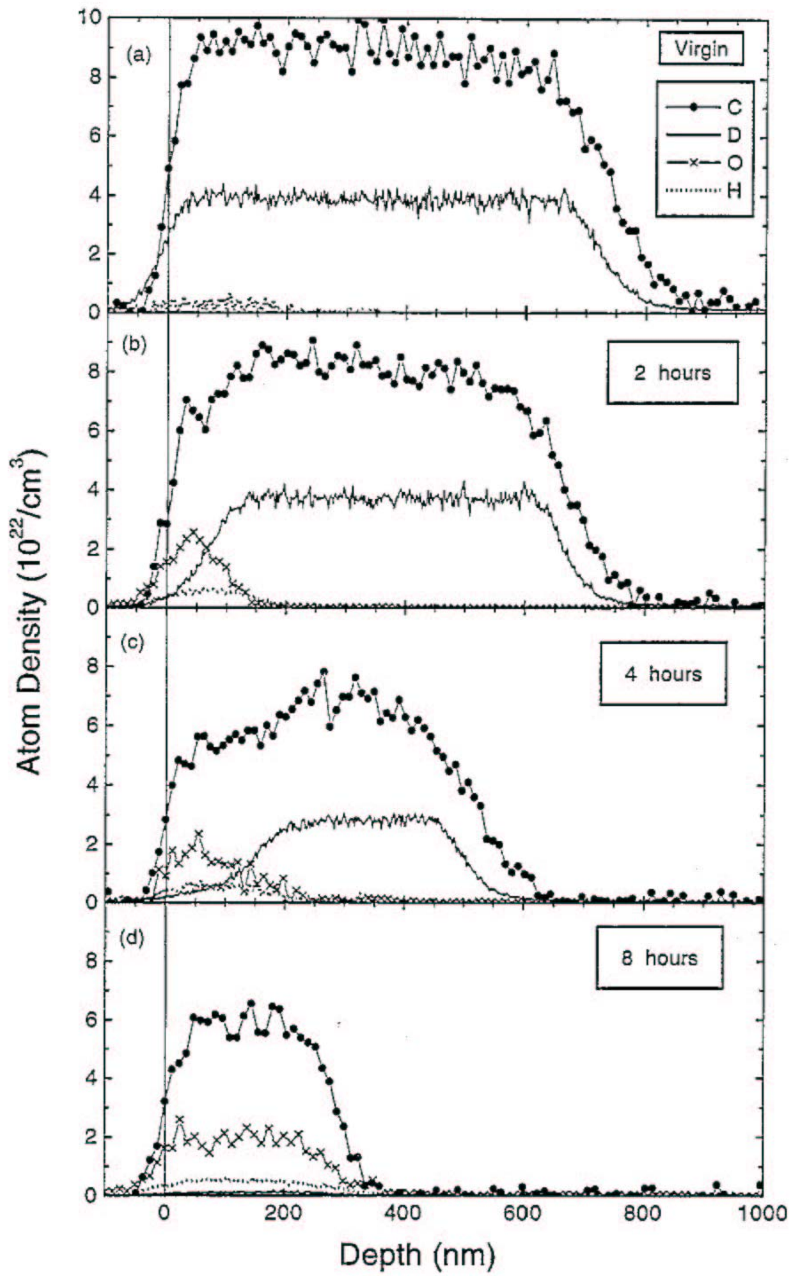

From Wang, 1997

Thermal Oxidation: Lab Results 2

2) Carbon is removed primarily as CO_2, hydrogen as H_2O.

$\Rightarrow$ Figure (Haasz, 1996)

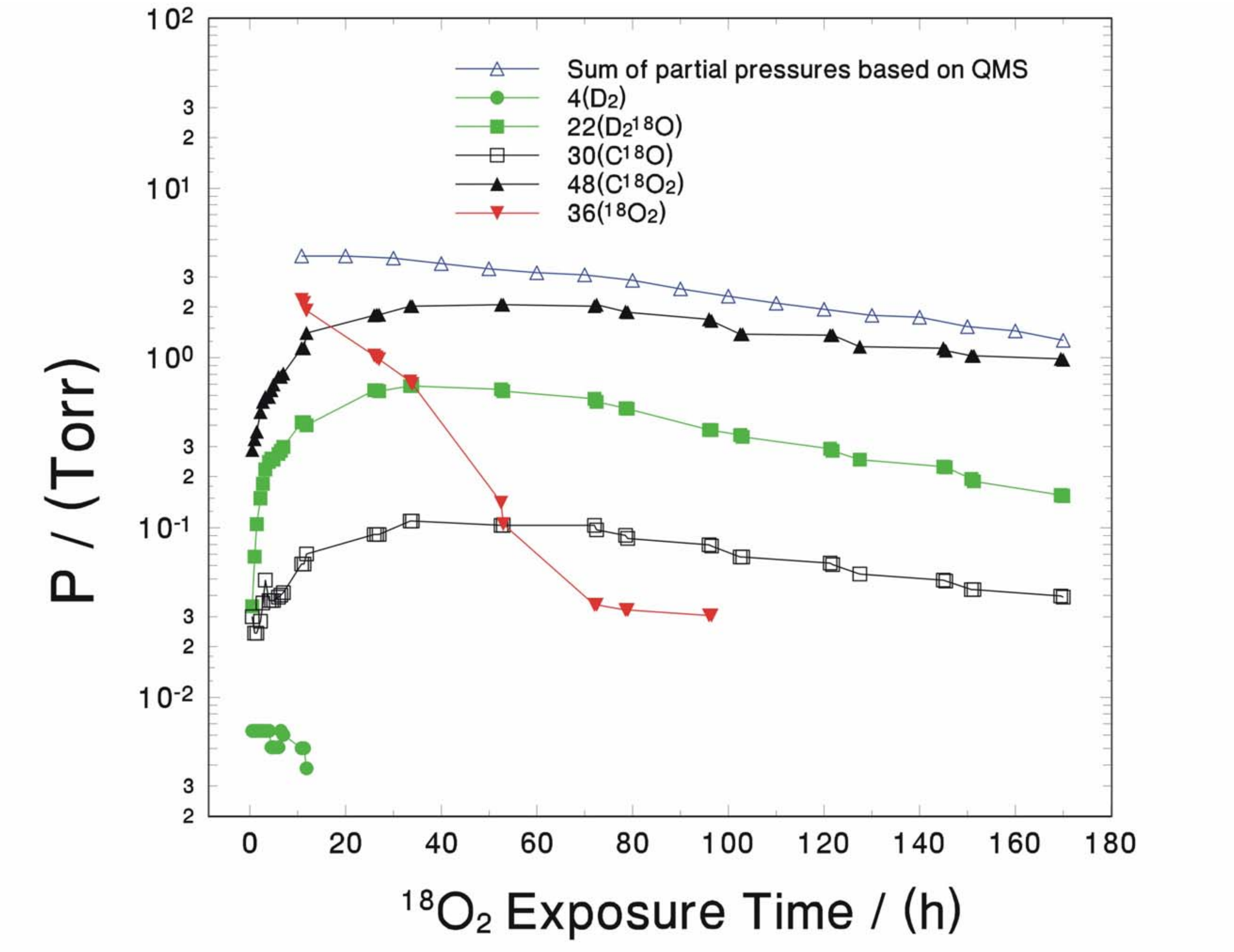

Sum of partial pressures based on QMS
4(D2)
22(D2 18O)
30(C18O)
48(C18O2)
36(18O2)
P / (Torr)
18O2 Exposure Time / (h)

Thermal Oxidation: Lab Results 3

- Film removal rates are strongly temperature dependent.
- Erosion rates > 50 μm/hr have been observed (Causey, 1990).
- Oxidation rates strongly dependent on film structure and impurity content.
- Oxidation of graphite substrates is negligible at temperatures of interest.

$\Rightarrow$ Figure (Davis, 2001b)

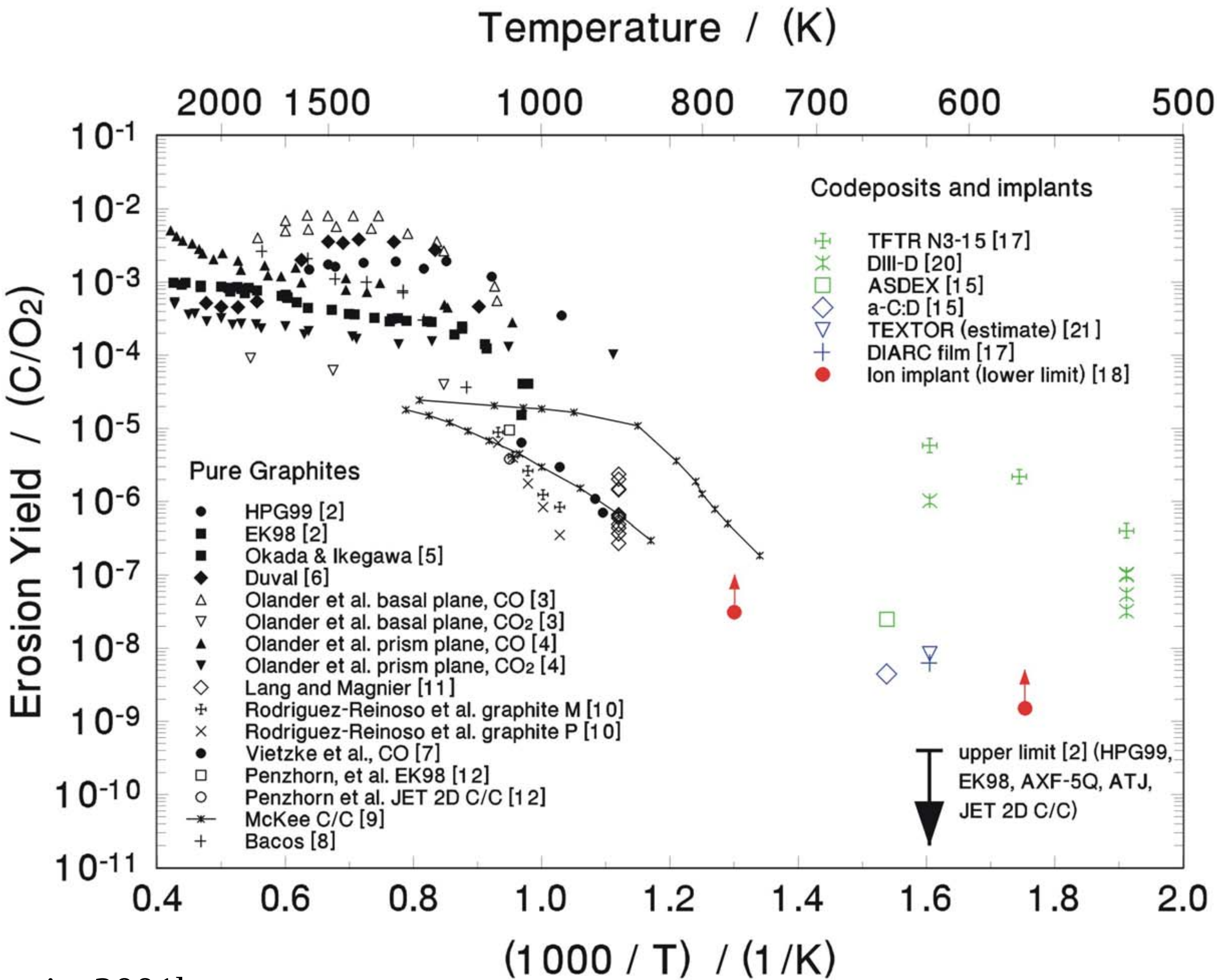

From Davis, 2001b

Thermal Oxidation: Tokamak Experience 1

- Deliberate exposure of a tokamak to oxygen during an operational phase has been tried on the TEXTOR tokamak (Philipps, 1999).

- Up to 0.2 Torr O_2 was allowed into the torus with the walls at 620 K.

- The formation of CO and CO_2 were observed as carbon codeposits were oxidized.

- Normal operation was recovered after a short period of conditioning.

$\Rightarrow$ However, there is no Be in TEXTOR, and the gettering of oxygen by Be is one of the main concerns.

Thermal Oxidation: Tokamak Experience 2

- More recently, oxidation experiments have taken place in HT-7 (China) and ASDEX-U.
  - In HT-7, a comparison was made of three oxidation techniques: thermo-oxidation, glow discharge oxidation, and ion-cyclotron resonance discharges (Hu, 2006).
  - In ASDEX-U, glow discharge oxidation was used (Hopf, 2006).
- In addition, both JET and DIII-D have experience accidental thermo-oxidation events when: a He bottle was not connected (JET) and a window broke during baking (DIII-D).
  - In both cases, recovery of plasma operation was obtained in a reasonable period of time, and no other detrimental effects were noted.

5.2.2 Plasma-Assisted Oxidation 1

- Several methods have been suggested for plasma-assisted oxidation:

1) Glow discharges in He/O_2

$\Rightarrow$ B field must be turned off

2) ECRF or ICRF discharges

$\Rightarrow$ can be done with B field on

Plasma-Assisted Oxidation 2

- Advantages:

  ⇒ Higher removal rates

  – This was clearly observed in the HT-7 experiments (Hu, 2006)

  ⇒ Less need for elevated temperatures

- Disadvantages:

  ⇒ Requires oxygen in the reactor

  ⇒ Only cleans line-of-sight surfaces

  – No film removal from tile gaps and other hidden surfaces (Hopf, 2006)

5.2.3 Oxidation with Ozone

- Ozone, O_3, is more reactive than molecular oxygen, O_2, therefore lower temperatures may be used.

- Film removal rates of 1-2 μm/hour observed at 460 K (Moormann, 2000).

- Otherwise, has similar advantages and disadvantages to oxidation with O_2.
    - May cause more damage to other components.

5.3 Surface Heating Techniques

- Heat surfaces to > 1000 K to desorb hydrogen from carbon-based films

  $\Rightarrow$ Much lower temperatures (~ 650 K ??) may work for metal-based deposits.

- May be possible to do this with specially tailored tokamak discharges which might heat plasma-facing surfaces (Whyte, 2005):

  $\Rightarrow$ The introduction of a radiating element to the plasma can quickly deposit most of the plasma energy reasonably uniformly over all plasma-facing surfaces.

- Hidden, or remote surfaces may require special heaters.

Local Heating Techniques

- The principle is to heat a small region of the surfaces to thermally desorb hydrogen, or to ablate the entire film.
- Trials have been done using a pulsed laser, with mirrors to scan over large surfaces (Skinner, 2002).
- Main advantage of all surface heating techniques is that oxygen is not required.
- Disadvantages of the laser technique are that only surfaces accessible to the laser can be cleaned; not between or behind tiles. Also, ablated films may redeposit elsewhere in the reactor.

5.4 Mechanical Scrubbing

- Grit blasting with an air or liquid carrier (Counsell, 2001)
- Requires a mechanism for removing the grit/removed film.

  $\Rightarrow$ Drains for liquids

  $\Rightarrow$ Conveyer belts for dry particulates

- May add greatly to the complexity of the remote maintenance machinery.

  $\Rightarrow$ One might imagine a team of miniature robots with scrub brushes and vacuum cleaners sent into the torus.

6. Conclusions

- Codeposition is likely to be the greatest source of tritium inventory in next-generation fusion reactors like ITER.
- Long-term inventories must be reduced by about two orders of magnitude, as compared to the experience in JET and TFTR.
- Specific technology and procedures will need to be developed in order to achieve this goal.
- Codeposition rates in a mixed material machine, like ITER, are subject to large uncertainties.

CHAPTER 1 REFERENCES

Federici, 2001: G. Federici, C. H. Skinner, et al., "Plasma-material interactions in current tokamaks, and their implications for next-step fusion reactors", Nucl. Fusion 41 (2001) 1967.

Federici, 2003: G. Federici, et al., "Key ITER plasma edge and plasma-material interaction issues", J. Nucl. Mater. 313-316 (2003) 11.

CHAPTER 2 REFERENCES

Thompson, 1968: M. W. Thompson, Philos. Mag. 18 (1968) 377.

Greenwood, 2002: J. Greenwood, "The correct and incorrect generation of a cosine distribution of scattered particles for Monte-Carlo modelling of vacuum systems", Vacuum 67 (2002) 217.

Marion, 2006: J. Marion, et al., "Characterization of Sputtered Products during Graphite Exposure to Deuterium Ions by molecular Dynamics", to be published.

Stangeby, 2000: P. C. Stangeby, "The Boundary Plasma of Magnetic Fusion Devices", Institute of Physics Publishing, Bristol, 2000.

Lisgo, 2003: S. Lisgo, "Interpretive modeling of the Alcator C-Mod Divertor", Ph. D. Thesis, University of Toronto, 2003.

Rubel, 2003: M. Rubel, et. al., "Beryllium and carbon films in JET following D-T operation", J. Nucl. Mater. 313-316 (2003) 321.

Wampler, 2006: W. R. Wampler, et al., "Transport and Deposition of 13C From Methane Injection Into Partially Detached Divertor H-mode Plasmas in DIII-D", 17th PSI conference, Hefei, 2006.

CHAPTER 3 REFERENCES

Haasz, 1999: A. A. Haasz, M. Poon and J. W. Davis, "The Effect of Ion Damage on Deuterium Trapping in tungsten", J. Nucl. Mater. 266-269 (1999) 520.

Jacob, 1998: W. Jacob, "Surface reactions during growth and erosion of hydrocarbon films", Thin Solid Films 326 (1998) 1.

Mills, 1989: B. E. Mills, D. A. Buchenaeur, A. E. Ponteau and M. Ulrickson, "Characterization of deposition and erosion of the TFTR bumper limiter and wall", J. Nucl. Mater. 162-164 (1989) 343.

Wright, 2003: P. B. Wright, J. W. Davis, et al., “Chemical erosion of DIII-D divertor tile specimens:, J. Nucl. Mater. 313-316 (2003) 158.

Federici, 2001: G. Federici, C. H. Skinner, et al., “Plasma-material interactions in current tokamaks, and their implications for next-step fusion reactors”, Nucl. Fusion 41 (2001) 1967.

Von Seggern, 1999: J. Von Seggern, et al., Physica Scripta T81 (1999) 31.

Causey, 1998: R. A. Causey and D. S. Walsh, “Codeposition of deuterium with beryllium”, J. Nucl. Mater. 254 (1998) 84.

Mayer, 1997: M. Mayer, “Codeposition of deuterium with BeO at elevated temperatures”, J. Nucl. Mater. 240 (1997) 164.

Markin, 2000: A. V. Markin et al., “Codeposition of deuterium ions with beryllium oxide at elevated temperatures”, J. Nucl. Mater. 283-287 (2000) 1094.

Baldwin, 2005: M. J. Baldwin, K. Schmid, R. P. Doerner, et al., “Composition and Hydrogen Isotope Retention analysis of Co-Deposited C/.Be Layers”, J. Nucl. Mater. 337-339 (2005) 590.

Krieger, 2003: K. Krieger, A. Geier, et al., “Erosion and migration of tungsten employed at the main chamber first wall of ASDEX Upgrade”, J. Nucl. Mater. 313-316 (2003) 327.

CHAPTER 4 REFERENCES

Vietzke, 1996: E. Vietzke and A. A. Haasz, “Chemical Erosion” in *Physical Processes of the Interaction of Fusion Plasmas with Solids*, Eds. W. O. Hofer and J. Roth , Academic Press, San Diego, 1996.

von Keudell, 1999: A. von Keudell, C. Hopf, T. Schwarz-Selinger and W. Jacob, “Surface loss probabilities of hydrocarbon radicals on amorphous hydrogenated carbon film surfaces: consequences for the formation of re-deposited layers in fusion experiments:, Nucl. Fusion 39 (1999(1451.

Garcia-Rosales, 1992: C. Garcia-Rosales and J. Roth, “Chemical sputtering of pyrolytic graphite and boron doped graphite USB15 at energies between 10 and 1000 eV”, J. Nucl. Mater. 196-198 (1992) 573.

Davis, 1998: J. W. Davis and A. A. Haasz, “Chemical erosion of CKC TiB_2-doped graphite”, J. Nucl. Mater. 255 (1998) 214.

Krieger, 2001: K. Krieger and J. Roth, “Synergistic effects by simultaneous bombardment of tungsten with hydrogen and carbon”, J. Nucl. Mater. 290-293 (2001) 107.

Goldstrass, 1999: P. Goldstrass, W. Eckstein and Ch. Linsmier, “Erosion of beryllium and deposition of carbon and oxygen due to bombardment with C^+ and CO^+ ions”, J. Nucl. Mater. 266-269 (1999) 581.

Eckstein, 2000: W. Eckstein, “Dynamic behaviour of the systems Be-C, Be-W and C-W”, J. Nucl. Mater. 281 (2000) 195.

Poon, 2000: M. Poon, J. W. Davis and A. A. Haasz, “Effect of carbon pre-implantation on deuterium retention in tungsten”, J. Nucl. Mater. 283-287 (2000) 1062.

CHAPTER 5 REFERENCES

Andrew, 1999: P. L. Andrew, et al., “Tritium retention and clean-up in JET”, Fus. Eng. Design 47 (1999) 233.

Federici, 2001: G. Federici, C. H. Skinner, et al., “Plasma-material interactions in current tokamaks, and their implications for next-step fusion reactors”, Nucl. Fusion 41 (2001) 1967.

Davis, 2001a: J. W. Davis, P. B. Wright, R. G. Macaulay-Newcombe, A. A. Haasz and C. G. Hamilton, “Chemical Erosion of Boronized films from DIII-D Tiles”, J. Nucl. Mater. 290-293 (2001) 66.

Wang, 1997: W. Wang, W. Jacob and J. Roth, “Oxidation and hydrogen isotope exchange in amorphous deuterated carbon films”, J. Nucl. Mater. 245 (1997) 66.

Haasz, 1996: A. A. Haasz, S. Chiu, J. E. Pierre and Y. I. Gudimenko, “Thermo-oxidative erosion of amorphous hydrogenated carbon films”, J. Vac. Sci. Technol. A14 (1996) 184.

Causey, 1990: R. A. Causey, W. R. Wampler and D. Walsh, “Comparison of the Thermal Stability of the Codeposited Carbon/Hydrogen Layer to that of the Saturated Implant Layer”, J. Nucl. Mater., 176&177 (1990) 987.

Davis, 2001b: J. W. Davis and A. A. Haasz, “Overview of thermo-oxidation of tokamak codeposits”, Physica Scripta T91 (2001) 33.

Philipps, 1999: V. Philipps et al., “Removal of redeposited layers and hydrogen release by oxygen ventilation of TEXTOR”, J. Nucl. Mater. 266-269 (1999) 386.

Hu, 2006: J. S. Hu, J. G. Li, X. M. Wang, Y. P. Zhao, et al., “Oxidation for Deposits Removal and Hydrogen Releasing on HT-7”, 17th PSI conference, Hefei, 2006.

Hopf, 2006: C. Hopf, V. Rohde, W. Jacob, et al., “Oxygen Glow Discharge Cleaning in ASDEX Upgrade”, 17th PSI conference, Hefei, 2006.

Moormann, 2000: R. M. Moormann, H. K. Hinssen and C. H. Wu, “Oxidation of carbon based first wall materials for ITER”, 18th IAEA Fusion Energy Conf., Sorrento, Italy, Oct. 4-10, 2000.

Whyte, 2005: D. G. Whyte and J. W. Davis, “Tritium Recovery in ITER by Radiative Plasma Terminations”, J. Nucl. Mater. 337-339 (2005) 560.

Skinner, 2002: C. H. Skinner, et al., “Tritium removal from JET and TFTR tiles by a scanning laser”, J. Nucl. Mater. 313-316 (2003) 496.

Counsell, 2001: G. F. Counsell and C. H. Wu, “In-situ detection and removal of carbon debris – a challenge for the next-step fusion device”, Physica Scripta T91 (2001) 70.